AD_____

Award Number: W81XWH-10-1-0347

TITLE: Innovative Strategy for Treatment of Lung Cancer: Inhalatory Codelivery of Anticancer Drugs and siRNA for Suppression of Cellular Resistance

PRINCIPAL INVESTIGATOR: Oleh Taratula, Ph.D.

CONTRACTING ORGANIZATION: Rutgers, The State University of New Jersey
New Brunswick, N.J. 08901-8559

REPORT DATE: July 2011

TYPE OF REPORT: Final

PREPARED FOR: U.S. Army Medical Research and Materiel Command
Fort Detrick, Maryland 21702-5012

REPORT DOCUMENTATION PAGE

Form Approved
OMB No. 0704-0188

1. REPORT DATE	2. REPORT TYPE	3. DATES COVERED
1 Jul 2011	Final	1 JUL 2010 - 30 JUN 2011

4. TITLE AND SUBTITLE

Innovative Strategy for Treatment of Lung Cancer: Inhalatory Codelivery of Anticancer Drugs and siRNA for Suppression of Cellular Resistance

5a. CONTRACT NUMBER

5b. GRANT NUMBER
W81XWH-10-1-0347

5c. PROGRAM ELEMENT NUMBER

6. AUTHOR(S)

Oleh Taratula, Ph.D.

E-Mail: olehtaratula@gmail.com

5d. PROJECT NUMBER

5e. TASK NUMBER

5f. WORK UNIT NUMBER

7. PERFORMING ORGANIZATION NAME(S) AND ADDRESS(ES)

Rutgers, The State University of New Jersey
New Brunswick, N.J. 08901-8559

8. PERFORMING ORGANIZATION REPORT NUMBER

9. SPONSORING / MONITORING AGENCY NAME(S) AND ADDRESS(ES)
U.S. Army Medical Research and Materiel Command
Fort Detrick, Maryland 21702-5012

10. SPONSOR/MONITOR'S ACRONYM(S)

11. SPONSOR/MONITOR'S REPORT NUMBER(S)

12. DISTRIBUTION / AVAILABILITY STATEMENT
Approved for Public Release; Distribution Unlimited

13. SUPPLEMENTARY NOTES

14. ABSTRACT

Themainobjectiveoftheproposedresearchisthedevelopmentofanoveldrugdeliverysystem(DDS)forinhalationtherapywhichisableto(1)provideinhalatorylungdeliveryofactivecomponents;(2)suppresspumpandnonpumpresistances;(3)providetargeteddrugdeliverytothecancercellsand(4)limitadversesideeffectsonhealthyorgans.Therefore,tofulfillthefollowingtasks,wedevelopedananomedicineplatformbasedonMesoporousSilicaNanoparticles(MSNs)forinhalationlocaldeliveryofanticancerdrugssuchasDoxorubicinandCisplatinincombinationwithMRP1andBCL2targetedsiRNAsassuppressorsofcellularresistance,respectively.Thiol-functionalizedMSNsweresynthesizedbyusingasurfactant-templated,base-catalyzedcondensationmethodbyfollowingpost-modificationofparticlesurface.Theporesofpreparedparticleshavebeenusedasreservoirsforstoringanticancerdrugs,whilethiol-functionalizedsiRNAsandpolyethyleneglycol(PEG)werechemicallyconjugatedtothesurfaceofMSNsviacleavabledisulfidebonds.Furthermore,LHRHpeptidewasattachedtothedistalendofPEGtodirecttheDDSspecificallytothelungcancercells.Invitrostudydemonstratedthefeasibilityofthedeveloped DDStosufficientlyenhancedeliveryofdrugsandsiRNAsintohumanA549lungcancercells.Furthermore,simultaneoussuppressionofmultidrugresistanceinlungcancercellssignificantlyenhancedtheapoptosisinductionactivityofanticanceragents.Moreover,inhalationco-deliveryofthedevelopedDDSintonudemicewithanorthotopicmodelofhumanlungcancersubstantiallyimprovedlungexposuretotheactivecomponentsandlimitedtheiraccumulationinotherorgan

15. SUBJECT TERMS
Lung cancer;Inhalation therapy;Chemotherapy;Multidrugresistance;siRNA;DrugDeliverySystem;Nanomedicine;Targetingdelivery;LHRH;MRP1;BCL

16. SECURITY CLASSIFICATION OF:			17. LIMITATION OF ABSTRACT	18. NUMBER OF PAGES	19a. NAME OF RESPONSIBLE PERSON
a. REPORT	b. ABSTRACT	c. THIS PAGE			USAMRMC
U	U	U	UU	75	19b. TELEPHONE NUMBER *(include area code)*

Table of Contents

Introduction

One of the main reasons for the poor survival rates among patients with lung cancer is the limited efficiency of traditional chemotherapy. The conventional treatments use high doses of toxic anticancer drugs which often produce severe adverse side effects on healthy organs [1]. Hence, an ideal anticancer therapy would involve the local administration of high drug concentration directly to the target tissue for the maximum treatment effect, limitation of drug degradation in the systemic circulation and low adverse side effects [2]. For lung diseases, aerosol technology had been developed to achieve this objective. However, the efficient aerosolized drug transfer is possible only for a limited number of drugs. In addition, the efficacy of chemotherapy is also limited by the rapid development of tumor resistance. The mechanisms of this resistance are common to most cancers and include "pump" and "nonpump" resistance [2]. Therefore, only simultaneous suppression of both pump and nonpump resistances is capable of substantial increasing in the efficacy of anticancer drugs. Consequently, **the main objective** of the proposed research is to mitigate resistance of lung cancer to chemotherapy through the development, characterization and in vivo evaluation of a novel drug delivery system (DDS) for inhalation therapy which contains five main components: (1) nanocarrier; (2) anticancer drugs; (3) suppressor of pump drug resistance; (4) suppressor of nonpump cellular resistance and (5) targeting moiety to the lung cancer cells. The nanomedicine platform based on Mesoporous Silica Nanoparticles (MSNs) has been developed for inhalation local delivery of anticancer drugs such as Doxorubicin (DOX) and Cisplatin (CIS) in combination with MRP1 and BCL2 targeted siRNAs as suppressors of cellular resistance, respectively. Thiol-functionalized MSNs were synthesized by using a surfactant-templated, base-catalyzed condensation method by following post-modification of particle surface. The pores of prepared particles have been used as reservoirs for storing anticancer drugs, while thiol-functionalized siRNAs and polyethylene glycol (PEG) were chemically conjugated to the surface of MSNs via cleavable disulfide bonds. Furthermore, LHRH peptide was attached to the distal end of PEG to direct the DDS specifically to the lung cancer cells.

BCL2: B-Cell Lymphoma 2 protein is an integral inner mitochondrial membrane protein responsible for cellular antiapoptotic defense. Overexpression of BCL2 blocks the apoptotic cell death.

MRP1: Multidrug resistance protein 1

Body

All the deadlines associated with three tasks outlined in the approved Statement of Work (Table 1) were met in time.

Table 1. Scope of work and timeline of the project.

Quarters		Q1				Q2				Q3			
Months		1	2	3	4	5	6	7	8	9	10	11	12
Task 1. To synthesize MSN, modify their surface, encapsulate anticancer drugs, conjugate siRNA and characterize the resulting complex multifunctional DDS													
1a.	Synthesis of MSN	■	■										
1b.	Preparation of thiol-functionalized MSN	■	■										
1c.	Modification of MSN with thiol reactive group	■	■										
1d.	Characterization of MSN size and shape	■	■										
1e.	Evaluation of MSN surface area and pore size	■	■										
1f.	Encapsulation of anticancer drugs in MSN pores		■	■									
1g.	Modification of PEG with LHRH		■	■									
1h.	Conjugation of siRNA and PEG-LHRH to MSN		■	■									
1i.	Evaluation of anticancer drug release *in vitro*			■	■								
1j.	Evaluation of siRNA release *in vitro*			■	■								
Task 2. To evaluate *in vitro*, the effectiveness of the proposed DDS for the cell transfection and suppression both types of cellular resistance to chemotherapy													
2a.	Evaluation of DDS cytotoxicity on cancer cells				■	■							
2b.	Evaluation of DDS intracellular localization				■	■							
2c.	Testing of drug and siRNA accumulation in cells				■	■							
2d.	Evaluation of MRP1 and BCL2 gene suppression				■	■	■						
Task 3. To select and characterize an optimal regimen of aerosol generation, nebulizer performance, droplet size and dose, dynamic stability of MSN based DDS and body distribution of airborne nanoparticles *in vivo*													
3a.	Testing of DDS stability after aerolization						■	■					
3b.	Developing of *in vivo* aerolization procedure								■	■			
3c.	Evaluation of MTD of the prepared DDS on mice								■	■	■		
3d.	Preparation of mice with lung tumor								■	■			
3e.	Evaluation of DDS accumulation in living mice									■	■		
3f.	Evaluation of DDS accumulation in mice organs									■	■		
3g	Estimation of adverse side effects for treatment											■	■

Task 1. To synthesize MSN, modify their surface, encapsulate anticancer drugs, conjugate siRNA and characterize the resulting complex multifunctional drug delivery system (DDS) (months 1-4):

Herein, we report the synthesis of a targeted DDS for pulmonary co-delivery of anticancer drugs and suppressors of multidrug cellular resistance that is based on Mobile Crystaline Material-41 (MCM-41) type of mesoporous silica nanoparticles. The MSN as drug delivery cargoes were

synthesized and consequently modified with (3-Mercaptopropyl)trimethoxysilane (MPTS) and Aldrithiol-2 to introduced pyridyldithiol reactive groups for covalent conjugation of multidrug resistance suppressors, PEG and targeting ligands (Fig.1A and 1B). DOX and CIS were used as the anticancer drugs to be encapsulated inside of the pyridyldithiol-terminated MSN (Fig.1C and 1D). Finally, the surfaces of the drug-loaded MSN were covalently modified with siRNA and PEG-LHRH via disulfide linkages (Fig.1E and 1F).

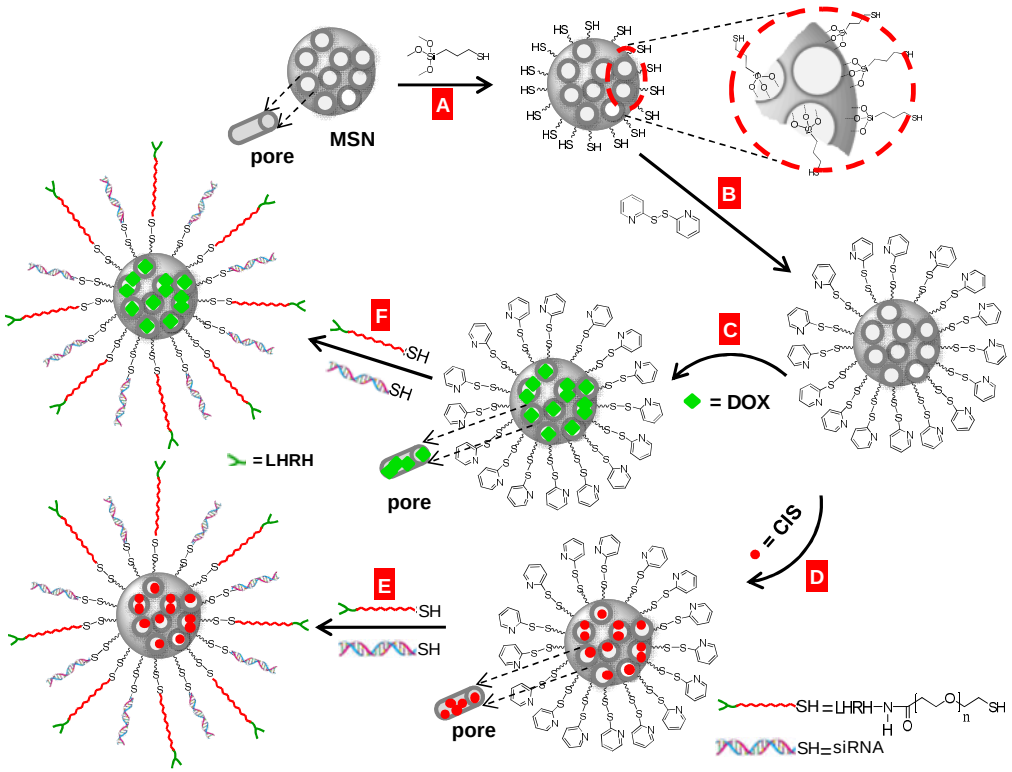

Figure 1. Surface engineered approach for the preparation of mesoporous silica nanoparticles (MSN) for an efficient targeted co-delivery of siRNA and anticancer drugs. (A) Modification of MSN with MPTS ; (B) Activation of thiol groups on the MSN surface with Aldrithiol-2 to produced pyridyldithiol reactive groups; (C) Encapsulation of DOX inside modified MSN; (D) Encapsulation of CIS inside modified MSN; (E) Modification of surface of DOX-loaded MSN with siRNA and PEG-LHRH; (F) Modification of surface of CIS-loaded MSN with siRNA and PEG-LHRH.

1a. *Synthesis of MSN (months 1-2)*

MSN as the drug carriers for inhalatory DDS were selected based on the following considerations. These nanoparticles have porous interiors that can be used as reservoirs for storing hydrophobic anticancer drugs and large surface areas that could be modified with siRNA and cell targeting moieties. The pore size can be tailored to selectively store different molecules

of interest, while the size of the particles can be tuned to maximize the efficiency of pulmonary delivery and cellular uptake[3]. In addition, a biodegradation product of MSN, orthosilicic acid, is natural compound with low toxicity found in numerous human tissues[4].
MCM-41 type of MSN was synthesized by using a surfactant-templated, base-catalyzed condensation method as previously described[3]. 0.5 g of N-Cetyltrimethylammonium bromide (CTAB) was dissolved in 240 ml of deionized (DI) water and then added with 1.75 ml of aqueous sodium hydroxide solution (2.00 M) in a 500ml round bottom flask. The temperature of the mixture was adjusted to 353 K and 2.50 ml of Tetraethoxysilane (TEOS) was added drop wise to the flask under vigorous stirring. The reaction was allowed to proceed for 2 h to give rise to white precipitate. The resulting product was filtered and washed with DI water and methanol, and dried at 60 °C under high vacuum to yield the as-synthesized MSN. To remove the surfactant template (CTAB), the as-synthesized MSN was refluxed for 17 h in a mixture of 1.5 ml of HCl (37.4 wt%) and 150.0 mL of methanol. The resulting material was filtered and extensively washed with H_2O and methanol. The surfactant-free MSNs were then dried under high vacuum at 60 °C overnight to remove the remaining solvent from the pores.

1b. *Preparation of thiol-functionalized MSN (months 1-2)*

The mercaptopropyl-derivatized MSN were obtained by post-modification of as-synthesized MSN with MPTS, offering terminal thiol groups as reactive sites. Briefly, 0.40 ml of MPTS was added to 50 ml of anhydrous toluene in a flask. Then 400 mg of surfactant-free MSNs was added. After 24 h refluxing, the heating was stopped and the vessel was let to cool down to ~ 35 °C. The resulting powder suspension was then centrifuged at 10000 rpm for 20 min to remove the free MPTS and toluene. Then the precipitate was rinsed with toluene and anhydrous methanol. Thus-obtained powder was dried under vacuum at 75 °C overnight to remove any remaining solvent. Ellman's reagent was employed to quantify the concentration of thiol groups on the surface of MSNs accessible for further modification[5]. An average of 302.1 nmoles of thiols was measured per 1 mg of MSNs via standardization versus MPTS.

1c. *Modification of MSN with thiol-reactive groups (months 1-2)*

In order to conjugate siRNA and PEG via disulfide linkages, the thiol groups on the surface of MSNs were first reacted with 2,2'-Dipyridyl disulfide (Aldrithiol-2) to produced pyridyldithiol reactive groups. Briefly, 250 mg of MPTS-MSN in 25 mL methanol were added drop wise to a solution containing 0.55 g of Aldrithiol-2, 0.2 mL of glacial acetic acid, and 10 mL of methanol. After the reaction within 24 h at room temperature, the mixture was centrifuged at 10 000 rpm for 20 min to purify pyridylthiol-terminated MSN. Then the precipitate was rinsed with methanol and dried under vacuum at 75 °C overnight to remove any remaining solvent. According to Ellman's reagent assay, after reaction with Aldrithiol-2 the free thiol groups on MSN surface were non-detected, which represent a fact that majority of functional groups were activated and available for further conjugation with siRNA and PEG via reversible disulfide bond.

1d. *Characterization of MSN size and shape (months 1-2)*

Thus, as-synthesized MSNs and surface modified MSN were characterized by Transmission Electron Microscopy (TEM), which showed a near spherical morphology with a hexagonal array of mesoporous channels (Fig. 2A and B). Additionally, the Dynamic Light Scattering (DLS) analysis revealed that as-synthesized MSN and MPTS-MSN had a uniform size around 160 nm with relatively low dispersion (Fig 2C).

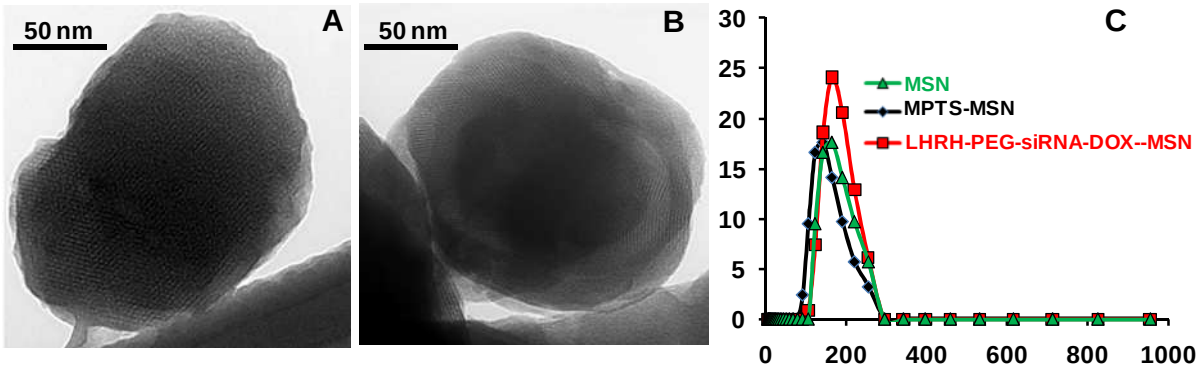

Figure 2. Characterization of mesoporous silica nanoparticles (MSN). Transmission electron microscope image of (A) as-synthesized MSN and (B) MPTS modified MSN. (C) Size distribution of as-synthesized MSN, MPTS-MSN and LHRH-PEG-siRNA-DOX-MSN measured by DLS.

1e. *Evaluation of MSN surface area and pore size (months 1-2)*

Furthermore, the surface areas, pore volumes, and pore size distributions of MSNs were respectively analyzed by nitrogen adsorption/desorption techniques using ASAP 2020 (Micromeritics)[3]. The Brunauer-Emmett-Teller (BET) surface area, pore size and pore volume, determined based on Barret-Joyner-Halenda (BJH) model, are summarized in Table 2. As-synthesized MSNs have a mean pore size of 2.99 nm, surface area of 1001 m^2/g, and pore volume of 1.0 cm^3/g. As a result of MSN modification with MPTS, the surface area, pore volume and pore size of MPTS-MSNs were all decreased to 821 m^2/g, 0.65 cm^3/g and 2.83 nm, respectively (Table 2).

Table 2. The Brunauer-Emmett-Teller (BET) surface area, the pore size and pore volume determined based on Barret-Joyner-Halenda (BJH) model. Means ± SD are shown.

Nanoparticle	BET surface area (m^2/g)	BJH pore volume (cm^3/g)	BJH pore size (nm)
MSN	1001 ±8	1.00 ±0.12	2.99 ±0.11
MPTS-MSN	821 ±5	0.65 ±0.06	2.83 ±0.08

1f. *Encapsulation of anticancer drugs in MSN pores (month 2-3)*

The selection of anticancer drugs was based on the following considerations. First, the drugs should be currently used in clinics for treatment of resistant small cell lung cancer. Secondly, these drugs should be substrates for drug efflux pumps. This will allow for experimental assessment of pump suppression by the proposed DDS. Additionally, recent clinical studies demonstrated that combinations of the anticancer drugs result in a more efficient tumor regression compared to either drug alone[6]. Consequently, a mixture of DOX and CIS as the anticancer agents was selected for treatment of lung cancer via pulmonary route. In order to load DOX into the pores of MSNs, our previously developed procedure was employed in the current study[3]. Briefly, pyridyldithiol-terminated MSNs were suspended in a DOX solution in 3:5 (v:v) MeOH:H_2O co-solvent under continuous stirring for 24 hr. The loading efficiency of doxorubicin into MSNs pores was determined by measuring changes in optical absorption of the feeding solution and supernatants at 490 nm. Then the difference between concentration of the drug in feeding solution and supernatant was used to evaluate the amount of DOX loaded into the MSNs. The encapsulation efficiency (weight ratio of DOX loaded into MSNs to MSNs, w/w %) was determined to be approximately 8%. Additionally, to encapsulate CIS into the pores of nanoparticles, previously reported procedure was employed in the current study[7]. Briefly, pyridyldithiol-terminated MSNs were resuspended in CIS solution in 1:1 H_2O-DMSO co-solvent (v:v) under continuous stirring for 24 hrs. After centrifugation of MSN-CIS complexes, drug loading efficiency was determined by using a modified colorimetric assay based on the reaction of platinum with OPDA[8]. It was found that CIS loading efficiency was reasonably high up to 30% as compare to DOX encapsulation into pyridyldithiol-terminated MSNs.

1g. *Modification of PEG with LHRH (month 2-3)*

In order to enhance steric stability of DDS and reduce their uptake by cells of reticuloendothelial system, heterobifunctional PEG was employed to modify the MSNs surface with hydrophilic polymers. Moreover, the cytotoxic effect of chemotherapy on healthy organs can also be limited by employing the DDS with a ligand that specifically targeted to receptors overexpressed in the plasma membrane of cancer cells. Our previous study demonstrated that the receptors for LHRH peptide are overexpressed in cancer cells and are not expressed detectably in most visceral organs[9]. Taking advantage of this differential receptor expression, modified LHRH peptide was

selected as targeting moiety on the proposed DDS to enhance drug uptake specifically by the lung cancer cells and reduce the relative availability of the toxic drug to normal cells. The sequence of LHRH peptide was modified to provide a reactive amino group only on the side chain of a lysine residue. Therefore, primary amine of LHRH was first reacted with activated carboxylic group of heterobifunctional HOOC-PEG-SH. Briefly, the LHRH analogue was reacted with one equivalent of HS-PEG-COOH, in a mixture of anhydrous DMSO and DCM (3:5, v/v). Equimolar amount of EDC·HCl, was added as a coupling agent and DMAP was used as a catalyst. Triethylamine base was added to remove the salt from coupling agent. The reaction was stirred continuously for 24 h at room temperature. The resulting solution was filtered to remove dicyclohexylurea (DCU) and the filtrate was dialyzed extensively with DMSO and DI water (dialysis membrane of molecular weight cut off = 5 000 Da) for 24 h to remove unreacted LHRH peptide, EDC·HCl, DMAP and triethylamine. Further, the conjugate was lyophilized.

1h. Conjugation of siRNA and PEG-LHRH to MSN (month 2-3)

siRNA has been shown to be highly effective in suppressing the synthesis of different proteins[10-11]. In order to suppress pump and nonpump resistance of lung cancer cells and therefore substantially enhance antitumor efficiency of delivered drugs, two types of siRNA were conjugated with MSN nanoparticles. The first type of siRNA was targeted to MRP1 mRNA. It is known that this protein is mainly responsible for active efflux anticancer drugs (pump resistance) in non-small cell lung carcinoma[2]. The sequence of the siRNA targeted to MRP1 mRNA was: 5'-[S-S-C6]-GGC-UAC-AUU-CAG-AUG-ACA-CdTdT-3'(sense strand) and 5'-GUG-UCA-UCU-GAA-UGU-AGC-CdTdT--3'. The second type of siRNA was targeted to BCL2 mRNA. This protein plays a central role in antiapoptotic defence forming the basis for nonpump resistance in many cancer cell lines and inhibition of such cellular defence can be effectively used in order to enhance the efficiency of chemotherapy[2]. The sequence of the siRNA targeted to BCL2 mRNA were: 5'-[S-S-C6]-GUG-AAG-UCA-ACA-UGC-CUG-CdTdT-3' (sense strand) and 5'-GCA-GGC-AUG-UUG-ACU-UCA-CdTdT-3' (antisense strand). In order to visualize siRNA with fluorescence microscope, antisense strand was additionally modified with fluorescent dye: 5'-TAM-GCA-GGC-AUG-UUG-ACU-UCA-CdTdT-3'. Consequently, we expected that the use of siRNA targeted to MRP1 and BCL2 mRNA in the proposed DDS can provide for an effective suppression of both pump and nonpump cellular resistance and therefore enhance the effectiveness of anticancer drugs. To minimize the loss of RNAi activity, a thiol group was build into the sense strand of siRNA and was involved in the conjugation of siRNA to MSNs via a thiol/disulfide exchange reaction. Briefly, 2-pyridyl activated thiol groups on the MSN surface at concentration of 302.1 μM reacted with 10 μM of thiol groups on 5' end of siRNA sense strand targeted either to BCL2 or MRP1 mRNAs. To determine the efficiency of the conjugation method, the resulting siRNA-MSNs were precipitated by centrifugation and the concentration of unconjugated siRNA in supernatant was evaluated by detecting emission of TAMRA dye on 5' end of an antisense strand. Calibration data was then employed to calculate the siRNA concentration left in the solution versus the covalently conjugated to the MSN surface. According to the obtained result, 80 % of siRNA molecules were covalently attached to MSN surface via disulfide linkage.

Furthermore, the purified LHRH-PEG-SH conjugates derivatized with a terminal sulfhydryl group were then added to the 2-pyridyl activated thiol groups on siRNA-Drug-MSN to obtain LHRH-PEG-siRNA-Drug-MSNs complex via a sulfhydryl exchange reaction. It worth to mentioned that only 2.6 % of the 2-pyridyl activated thiol groups (8.0 nmole out of 302.1 nmole/1 mg of MSNs) on MSN surface were used for conjugation of siRNA. Therefore, 97.4% (294.1 nmole/1mg of MSN) of the 2-pyridyl activated thiol groups were available for covalent attachment of LHRH-PEG-SH via disulfide linker.

The presence of LHRH peptide on the MSN surface was detected by BCA protein assay (Thermo Fisher Scientific Inc., Rockford, IL)[10]. The spectra of the product corresponding to free LHRH and LHRH modified MSNs have well defined absorbance maximum around 560 nm corresponding to the absorbance of the BCA/copper complex formed as a result of the reaction of BCA reagent with the cuprous cation produced from the reduction of Cu^{+2} to Cu^{+1} by the LHRH peptide (Fig. 3). This maximum is absent in the assay spectra of the PEG-siRNA-MSNs complexes that are not modified with LHRH (Fig 3). Additionally, DLS measurements revealed the fact that in comparison with non-modified MPTS-MSNs, the modified LHRH-PEG-siRNA-Drug-MSNs complex became slightly larger (from 160.0 nm to 180.0 nm for non-modified and modified nanoparticles) (Fig 2C). The increase in the size of the prepared nanoparticles could be attributed to the modification of their surfaces by PEG and the targeting LHRH peptide layer.

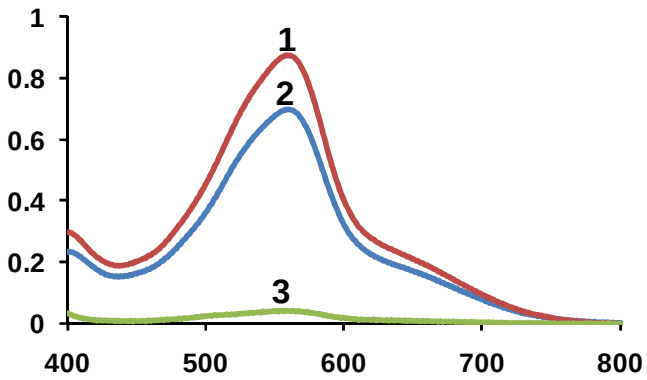

Figure 3. The typical absorption spectra of the product of BCA assay reaction with (1) free LHRH, (2) LHRH-PEG-siRNA-MSN and (3) PEG-siRNA-MSN.

1i. *Evaluation of anticancer drug release in vitro (months 3-4)*

Intrinsic fluorescence of DOX was employed in this study to evaluate a release of the drugs from LHRH-PEG-siRNA-Drug-MSNs complex. Briefly, the release of DOX from DDS was studied by suspending LHRH-PEG-siRNA-DOX-MSNs in either 10% water solution of human serum or 10% water solution of human serum containing 10 mM reduced glutathione at 37°C and the monitoring the fluorescence of the suspension at different time points. Since the fluorescence of DOX was completely quenched after loaded into MSN, the fluorescence of DOX in a suspension is solely due to release of DOX and was used to quantify the amount of released DOX based on

the fluorescence calibration curve of free DOX in 10% water solution of human serum. The DOX release profiles in both 10% water solution of human serum and 10% water solution of human serum containing 10 mM reduced glutathione as a function of release time are presented in Figure 4. According to Figure 4 the burst release in 10% water solution of human serum is 18.2%, while the presence of reduced glutathione in the incubation medium increased the burst release up to 35.3%. Furthermore, the release profile indicated that over a release time up to 96 hr, only 61% of DOX was released from LHRH-PEG-siRNA-DOX-MSNs complexes. On the other hand, the presence of 10 mM reduced glutathione facilitate the release rate of the drug at each time point and 93% of DOX was released from MSN based DDS after 96 hr. The observed phenomenon could be explained by the fact, that layer on the MSN surface formed by PEG-LHRH and siRNA inhibit the release of DOX from MSN pores. At the same time, the presence of reduced glutathione in the medium resulted in the cleavage of disulfide bonds, which conjugate PEG-LHRH and siRNA molecules to the MSN surface. As a result of disulfide bond cleavage, the layer formed by PEG-LHRH and siRNA around MSN is removed and the drug release rate is increased.

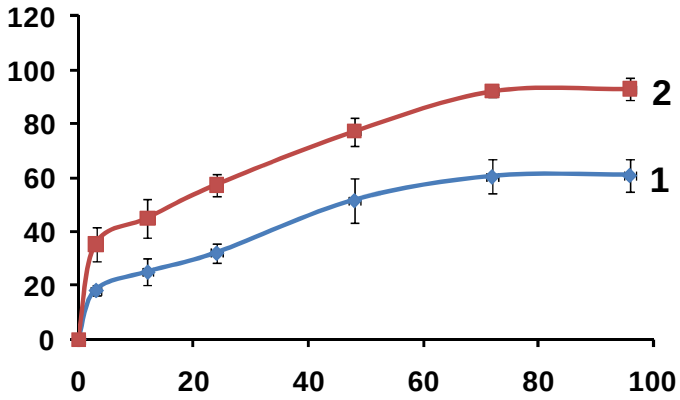

Figure 4. DOX release profile from LHRH-PEG-siRNA-DOX-MSNs complexes resuspended in either 10% water solution of human serum (1) or 10% water solution of human serum containing 10 mM reduced glutathione (2) at 37°C.

1j. *Evaluation of siRNA release in vitro (months 3-4)*

The disulfide bond introduced between the MSN and siRNA is an important factor for intracellular RNAi mechanism, because it is chemically labile and can be cleaved with cell-produced disulfide reducing agent such as reduced glutathione. To confirm that the disulfide bonds of siRNA-S-S-MSN could be cleaved under cellular reductive conditions, the prepared conjugates were incubated for 30 min with 10 mM water solution of reduced glutathione at 37C, which corresponds to the concentration of reduced glutathione in the cellular cytoplasm[12]. After centrifugation, the amount of siRNA in the supernatant was quantified by measuring emission of fluorescent dye (TAMRA) attached to an antisense strand as described above. The obtained data demonstrated that 98% of siRNA was released from siRNA-S-S-MSN complex in the presence of reduced glutathione. Based on the result, it is expected that the released siRNA could be

involved in the RNAi mechanism without any loss of their activity. It worth to mentioned, the antisense strands of siRNA used for *in vitro* and *in vivo* studies were not modified to conserve their biological functions.

Task 2. To evaluate *in vitro*, the effectiveness of the proposed DDS for the cell transfection and suppression both types of cellular resistance to chemotherapy (months 4-6):

In the present study, we describe novel complex multifunctional drug delivery systems suitable for simultaneous tumour targeted inhalation delivery of several anticancer drugs in combination with various types of siRNA. The proposed treatment approach includes inhalation of a mixture (a cocktail) of several DDS. Every single DDS consists of a carrier (modified mesoporous silica nanoparticles), an anticancer drug (doxorubicin or cisplatin), a suppressor of pump or nonpump resistance (siRNA targeted to MRP1 or BCL2 mRNA) and a tumour targeting moiety (LHRH peptide). Each individual component of DDS performs its specific function. A carrier binds all other components together ensuring high water "solubility" of entire complex and effective penetration via plasma membranes of targeted cancer cells. An anticancer drug induces apoptosis in lung caner cells. Suppressors of pump and nonpump resistance inhibit active drug efflux from cancer cells and their antiapoptotic defence, respectively, substantially enhancing antitumor efficiency of anticancer drugs. A tumour targeting moiety guarantees the uptake of an entire DDS with encapsulated drugs and siRNA specifically by cancer cells that express the corresponding receptor limiting adverse side effects on healthy lung cells. In addition, local inhalation delivery led to the preferential accumulation of delivered therapeutics mainly in the lungs and prevented the leakage of DDS and their components into the systemic circulation limiting adverse side effects of chemotherapy on healthy organs and tissues.

2a. *Evaluation of DDS cytotoxicity on cancer cells (months 4-5)*

Antitumor activities of the proposed MSN based DDS capable of co-delivery of anticancer drugs and siRNAs as the suppressors of multidrug cellular resistance in A549 human lung cancer cells were studied *in vitro* using a modified MTT assay[10]. Briefly, cancer cells were seeded into 96-well microtiter plates at the density of 10 000 cells per well. To measure cytotoxicity, cancer cells were separately incubated in 96-well plate with different concentrations of MSN formulations, which resulted in a total of five separate series of experiments: (1) MPTS-MSN; (2) LHRH-PEG-MSN; (3) Mixture of DOX and CIS (1:1, w/w); (4) Mixture of LHRH-PEG-DOX-MSN and LHRH-PEG-CIS-MSN (DOX/CIS = 1:1, w/w) and (5) Mixture of LHRH-PEG-siRNA(BCL2)-DOX-MSN, LHRH-PEG-siRNA(MRP1)-DOX-MSN, LHRH-PEG-siRNA(BCL2)-CIS-MSN and LHRH-PEG-siRNA(MRP1)-CIS-MSN (DOX/CIS = 1:1, w/w).
Cells were cultured for 24 h before the cell viability assay was performed. The old medium was removed and 100 µl of fresh medium and 25 µl of a 5 mg/mL MTT solution in DPBS were added to each well. Plates were then incubated under cell culture conditions for 3 h. 100 µl of 50% (v/v) DMF in water containing 20% (w/v) sodium dodecyl sulfate (with pH adjusted to 4.7 by acetic acid) were added to every well and incubated overnight to dissolve the formazan crystals. The absorbance of each sample was measured at 570 nm with a background correction at 630 nm using a conventional microtiter plate reader. On the basis of these measurements,

cellular viability was calculated for each concentration of the formulation tested. It was found that a mixture of free antitumor drugs such as CIS and DOX at 1:1 w/w ratio substantially limited the viability of the cancer cells and cytotoxicity of anticancer agents increased with drugs concentrations (Fig. 5B, line 3). Remarkably, the drugs mixture delivered by LHRH targeted DDS significantly enhanced their antitumor activity in the cancer cells (Fig. 5B, line 4).

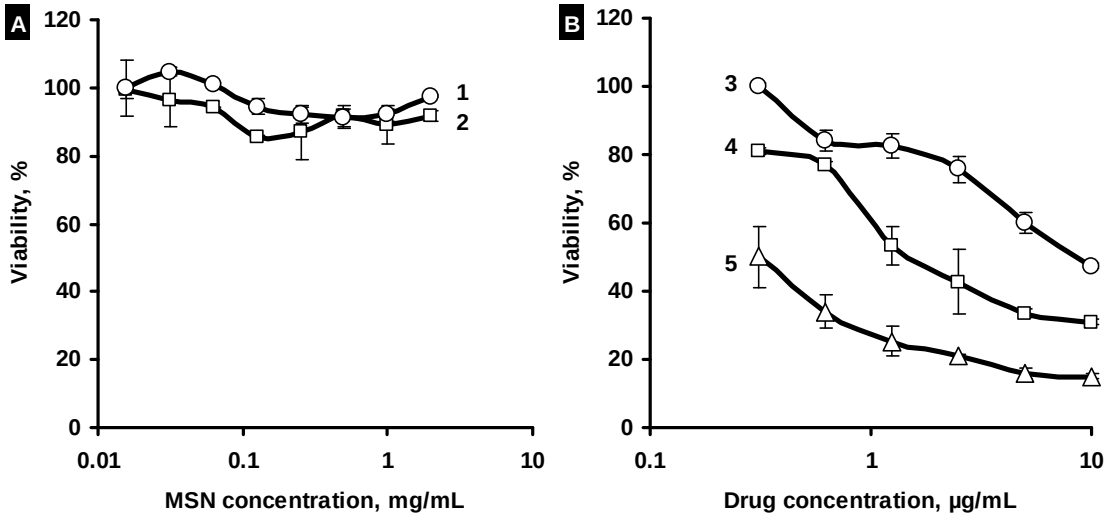

Figure 5. Cytotoxicity of different formulations: (A) Mesoporous silica nanoparticles (MSN) without drugs; (B) Different drug formulations. A549 human lung cancer cells were incubated within 24 h with different concentrations of indicated formulations: 1 - MPTS-MSN; 2 - LHRH-PEG-MSN; 3 - Mixture of DOX and CIS (1:1 w/w); 4 - Mixture of LHRH-PEG-DOX-MSN and LHRH-PEG-CIS-MSN (DOX:CIS = 1:1 w/w); and 5 - Mixture of LHRH-PEG-siRNA(BCL2)-DOX-MSN, LHRH-PEG-siRNA(MRP1)-DOX-MSN, LHRH-PEG-siRNA(BCL2)-CIS-MSN and LHRH-PEG-siRNA(MRP1)-CIS-MSN (DOX:CIS = 1:1 w/w). Means ± SD are shown.

According to MTT measurements, the IC_{50} dose (the dose that kills 50% of cells) of free drugs mixture (~9.0 µg/mL) was 6 times higher when compared to the mixture of CIS and DOX delivered by MSN based DDS (~1.5 µg/mL) specifically targeted to lung cancer cells. The sufficient enhancement in cytotoxicity of anticancer agents is not caused by MSNs alone since minimal toxicity for the drug-free nanoparticles at the employed concentrations was detected (Fig. 5A). The improved cytotoxicity of mixture of LHRH-PEG-DOX-MSN and LHRH-PEG-CIS-MSN can be explained by the possible higher accumulation of drugs inside the cells as demonstrated below. Furthermore, the mixture of four cancer LHRH targeted different DDS containing LHRH-PEG-siRNA(BCL2)-DOX-MSN, LHRH-PEG-siRNA(MRP1)-DOX-MSN, LHRH-PEG-siRNA(BCL2)-CIS-MSN, and LHRH-PEG-siRNA(MRP1)-CIS-MSN provides for a highest cytotoxic effect that cannot be achieved by either free drugs or drugs delivered by targeted MSN without siRNA (IC_{50}=0.3 µg/mL) (Fig. 5B, line 5). The ability of the siRNAs to sufficiently enhance *in vitro* antitumor activity of CIS and DOX could be explained by decreasing both pump and nonpump drug resistances of cancer cells against chemotherapy. Nonpump drug resistance is primarily attributed to the activation of antiapoptotic cellular

defense, and BCL2 protein is a key player in this defense. While the major drug efflux pump in non-small lung cancer cells is represented by MRP1 protein. The downregulations of genes expression responsible for both pump and nonpump resistance demonstrated below[2,10-11].

2b. *Evaluation of DDS intracellular localization (months 4-5)*

In order to test timed release of the active components of the prepared DDS and their intracellular localization by confocal microscopy, living A549 human lung cancer cells were separately incubated with LHRH-PEG-siRNA(TAMRA)-MSNs and LHRH-PEG-siRNA(non-labeled)-DOX-MSNs within 50 min. The siRNA was labeled with TAMRA (red fluorescence) and intrinsic fluorescence of DOX (red) was employed in the current study. The fluorescence of each dye was registered with a confocal microscope every 10 min and digitally photographed. It worth to mentioned that after loading into the pores of MSNs, DOX intrinsic fluorescence was completely quenched, which is in good agreement with our confocal microscopy images.

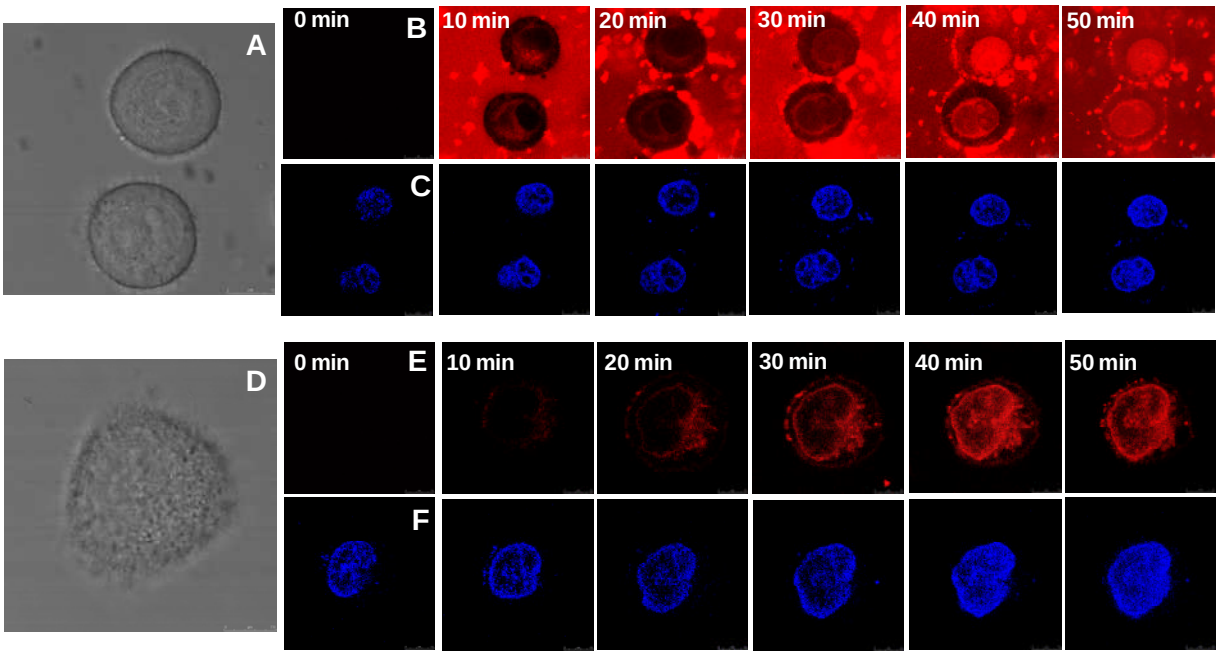

Figure 6. Cellular internalization of DOX and siRNA delivered by LHRH targeted MSN based DDS. Typical confocal microscopy images of living A549 human lung cancer cells incubated with (A-C) LHRH-PEG-siRNA(TAMRA)-MSN and (D-F) LHRH-PEG-siRNA(non-labeled)-DOX-MSN and recorded at different time points. A and D represent light images of A549 cells. B and E represent cellular localization of siRNA and DOX, respectively. C and F represent fluorescence images of nuclei stained with DAPI.

According to Figure 6E, DOX fluorescence was not detected around the cell while the drug was still encapsulated in MSN based DDS. On the other hand, siRNA fluorescence was observed in both extracellular and intracellular environments (Fig. 6B). The above mentioned feature enables

us to monitor the DOX release from MSN based DDS after cellular internalization. As one could observed in Figure 6B and 6E, siRNA and DOX fluorescence was detected after A549 cells incubation with LHRH-PEG-siRNA(TAMRA)-MSNs and LHRH-PEG-siRNA(non-labeled)-DOX-MSNs within 10 and 20 min, respectively. The 10 min delay in DOX internalization process could be explained by the fact that to record DOX fluorescence additional time is required for the drug to be release from MSN. Within 40 min of cells incubation with LHRH-PEG-siRNA(TAMRA)-MSNs and LHRH-PEG-siRNA(non-labeled)-DOX-MSNs complexes, both siRNA and DOX were sufficiently accumulated inside of the cells.
It worth to mentioned, that DOX was detected only in nucleus and perinuclear regions of cytoplasm, indicating efficient intracellular delivery and release of DOX from MSNs (Fig. 6 D-F). On the other hand, following internalization siRNA was localized in nucleus and cytoplasm of the cell (Fig. 6A-C). Since siRNA functions by binding to RNA-induced silencing complex in the cytoplasm, so that the delivery of siRNA to cytosol is important for further gene suppression[10-11].

2c. *Testing of drug and siRNA accumulation in cells (months 4-5)*

To determine intracellular accumulation of siRNA and anticancer agents into cancer cells, the cellular internalization of both TAMRA-labeled siRNA and DOX was investigated by fluorescence and confocal microscopy.

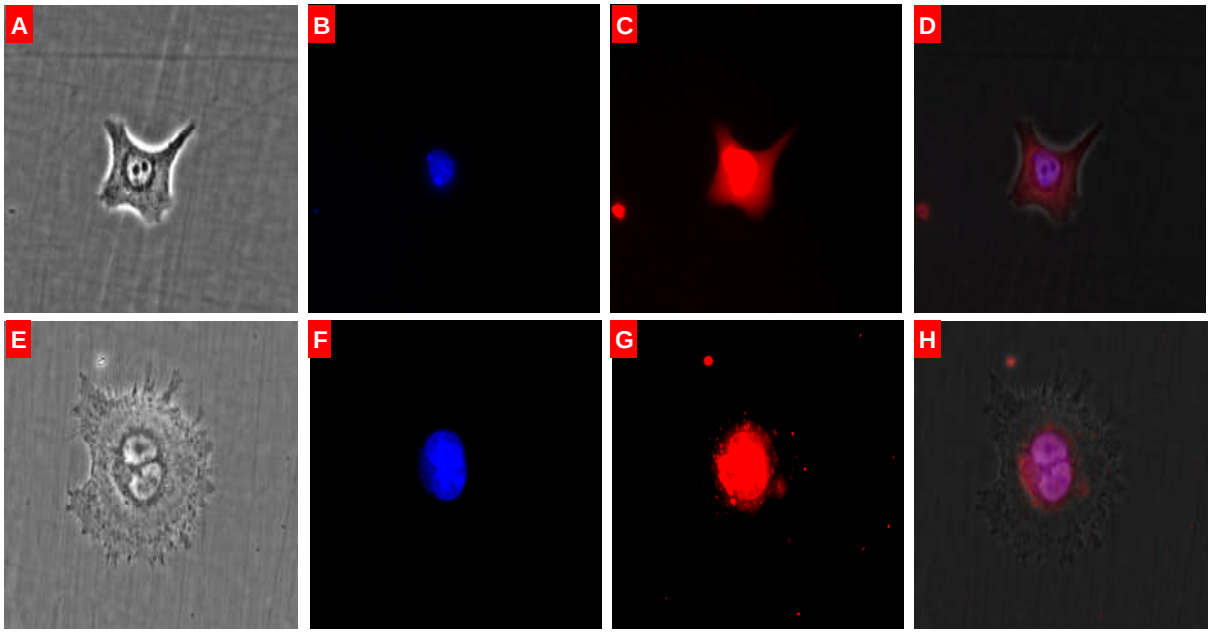

Figure 7. Representative fluorescent microscopy images of A549 human lung cancer cells incubated for 24 hrs with (A-D) LHRH-PEG-siRNA(TAMRA)-MSN and (E-H) LHRH-PEG-siRNA(non-labeled)-DOX-MSN . A and E represent light images of A549 cells; B and F represent fluorescence images of nuclei stained with DAPI. C and G represent cellular localization of siRNA and DOX, respectively. D and H are superposition of light and fluorescence images.

In the typical experiment, LHRH-PEG-siRNA(TAMRA)-MSNs and LHRH-PEG-siRNA(non-labeled)-DOX-MSNs were incubated with A-549 human lung cancer cell line for 24 hrs and the appropriate images were recorded with by fluorescence (Olympus America Inc., Melville, NY) microscope . According to Figure 7, the developed DDS is capable to efficiently facilitate transfer of both DOX and siRNA through the cellular membrane. As one could observe the intracellular accumulation pattern of siRNA and DOX detected by the above described confocal microscopy study was conformed by fluorescence microscopy experiment (Fig 7E-H). After incubation of A549 lung cancer cells with LHRH-PEG-siRNA(non-labeled)-DOX-MSNs complexes, red fluorescence was detected only in nucleus and perinuclear regions of cytoplasm (Fig 7E-H). On the other hand, siRNA was localized in both nucleus and cytoplasm of the cell (Fig. 7A-D).

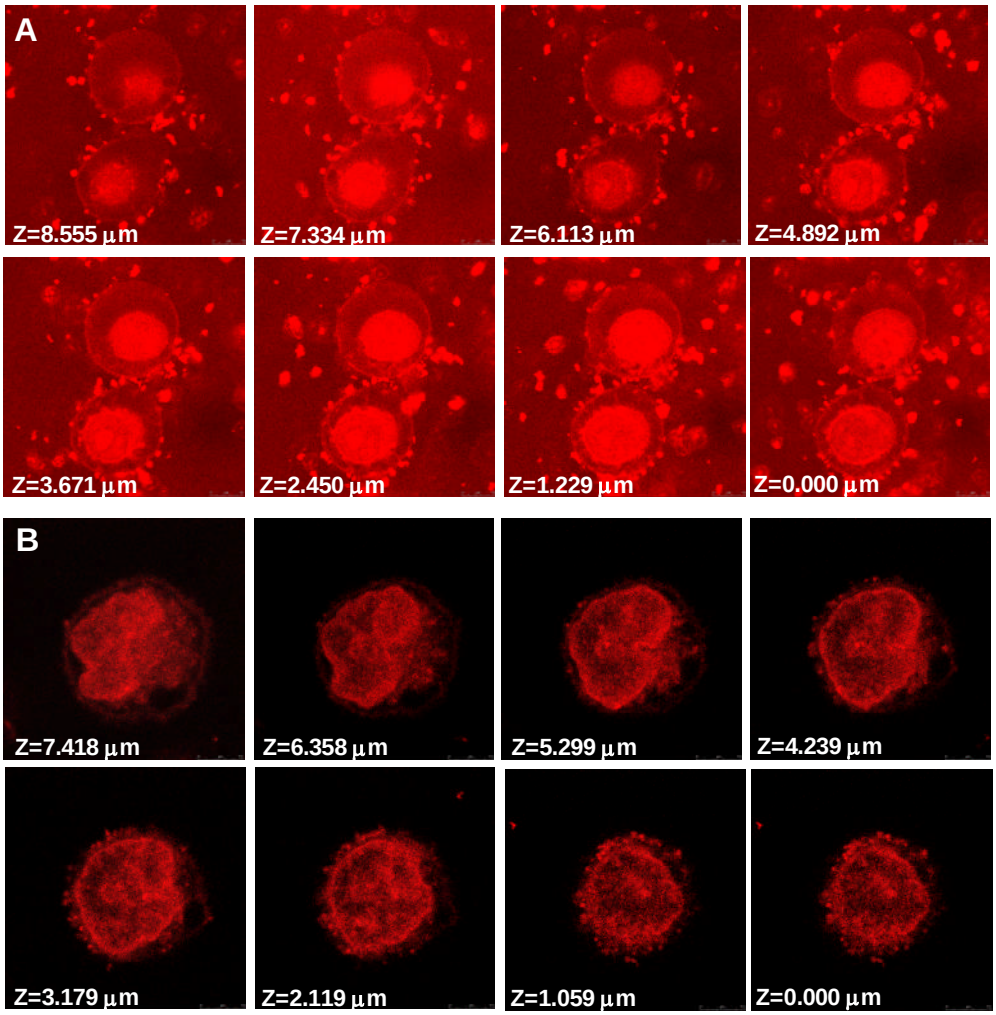

Figure 8. Confocal microscopy images (z-series from top to the bottom of the cells) of A549 human lung cancer cells incubated for 60 min with (A) LHRH-PEG-siRNA(TAMRA)-MSN and (B) LHRH-PEG-siRNA(non-labeled)-DOX-MSN.

Theoretically, DDS could adhere to the surface of cancer cells and erroneously be visualized on microscopic images as internalized within cells. To exclude such type of errors, we also analyzed the distribution of siRNA and DOX in different cellular layers from the upper to the lower of the fixed cell using confocal fluorescent microscopy (z-sections, Fig.8). The obtained data shows that distribution of siRNA and DOX was very similar in the different cell layers.

2d. *Evaluation of MRP1 and BCL2 gene suppression (4-6)*

The ability of the siRNAs molecules delivered by MSN to silence the targeted mRNA expression was investigated using quantitative reverse transcription-polymerase chain reaction (RT-PCR). RNA was isolated after 24 h incubation of A549 human lung cancer cells with (1) Control (fresh media); (2) Mixture of LHRH-PEG-DOX-MSN and LHRH-PEG-CIS-MSN, (3) Mixture of LHRH-PEG-siRNA(BCL2)-DOX-MSN, LHRH-PEG-siRNA(MRP1)-DOX-MSN, LHRH-PEG-siRNA(BCL2)-CIS-MSN and LHRH-PEG-siRNA(MRP1)-CIS-MSN (siRNA(BCL2): siRNA(MRP1) =1:1); and (4) Mixture of LHRH-PEG-siRNA(BCL2)-MSN and LHRH-PEG-siRNA(MRP1)-MSN (siRNA(BCL2): siRNA(MRP1) =1:1); using an RNeasy kit (Qiagen, Valencia, CA). The total concentration of siRNA was 0.20 μM. First strand cDNA was synthesized by Ready-To-Go You-Prime First-Strand Beads (Amersham Biosciences, Piscataway, NJ) with 4 mg of total cellular RNA and 100 ng of random hexadeoxynucleotide primer (Amersham Bioscience, Piscataway, NJ). After synthesis, the reaction mixture was immediately subjected to polymerase chain reaction, which was carried out using the GenAmp PCR System 2400 (Perkin-Elmer, Shelton, CT). PCR products were seperated in 4% NuSieve 3:1 Reliant agarose gels in 1(TBE buffer (0.089 M Tris/Borate, 0.002 M EDTA, pH 8.3; Research Organic Inc., Cleveland OH) by submarine gel electrophoresis. The gels were stained with ethidium bromide, digitally photographed, and scanned using the Gel Documentation System 920 (NucleoTech, San Mateo, CA). Gene expression was calculated as the ratio of mean band intensity of analyzed RT-PCR product (*BCL2*) or *(MRP1)* to that of the internal standard (B_2-*m*). The value of *BCL2 and MRP1* genes expression for untreated cells (control) was set to 100%. The results show that treatment of A549 human lung cancer cells with LHRH-PEG-siRNA(BCL2)-MSN and LHRH-PEG-siRNA(MRP1)-MSN (siRNA(BCL2): siRNA(MRP1) =1:1) complexes, which don't carry anticancer drugs, significantly influence the expression of the *BCL2* and *MRP1* genes after 24 hr. Thus, at the studied conditions, 56% and 58% silencing were achieved for *BCL2* and *MRP1* genes, respectively (Fig. 9A and 9B , Lines 4). The obtained data revealed the fact that siRNA molecules could be successfully released in cytoplasm from LHRH-PEG-siRNA-MSN complexes as a result of disulfide bond cleavage with reduced glutathione. Moreover, the released siRNAs are available for the formation of RISC complexes for further gene suppression. Furthermore, we demonstrated that incubation of A549 cancer cells with a mixture of LHRH-PEG-DOX-MSN and LHRH-PEG-CIS-MSN (DDS contain only anticancer drugs, no siRNA molecules) resulted in overexpression of *BCL2* and *MRP1* genes by ~20% in comparison to non-treated cells (Fig. 9A and 9B, Lines 2). Such phenomenon demonstrated a fact, that delivery of anticancer drugs into the cells caused an activation of both pump and non-pump cellular resistance through overexpression of *MRP1* and *BCL2* genes, respectively. On the other hand, a treatment of human lung cancer cells with LHRH targeted DDS, which carry both anticancer drugs and siRNA molecules (mixture of LHRH-PEG-

siRNA(BCL2)-DOX-MSN, LHRH-PEG-siRNA(MRP1)-DOX-MSN, LHRH-PEG-siRNA(BCL2)-CIS-MSN and LHRH-PEG-siRNA(MRP1)-CIS-MSN (siRNA(BCL2): siRNA(MRP1) =1:1)) resulted in downregulation of MRP1and BCL2mRNAs responsible for pump and nonpump cellular resistance by 50% and 35%, respectively (Fig.9A and 9B , Lines 3). Therefore, the highest cytotoxic effect of the proposed DDS that cannot be achieved by either free drugs or drugs delivered by targeted MSN without siRNA is related to simultaneous suppression of both types of cell resistance.

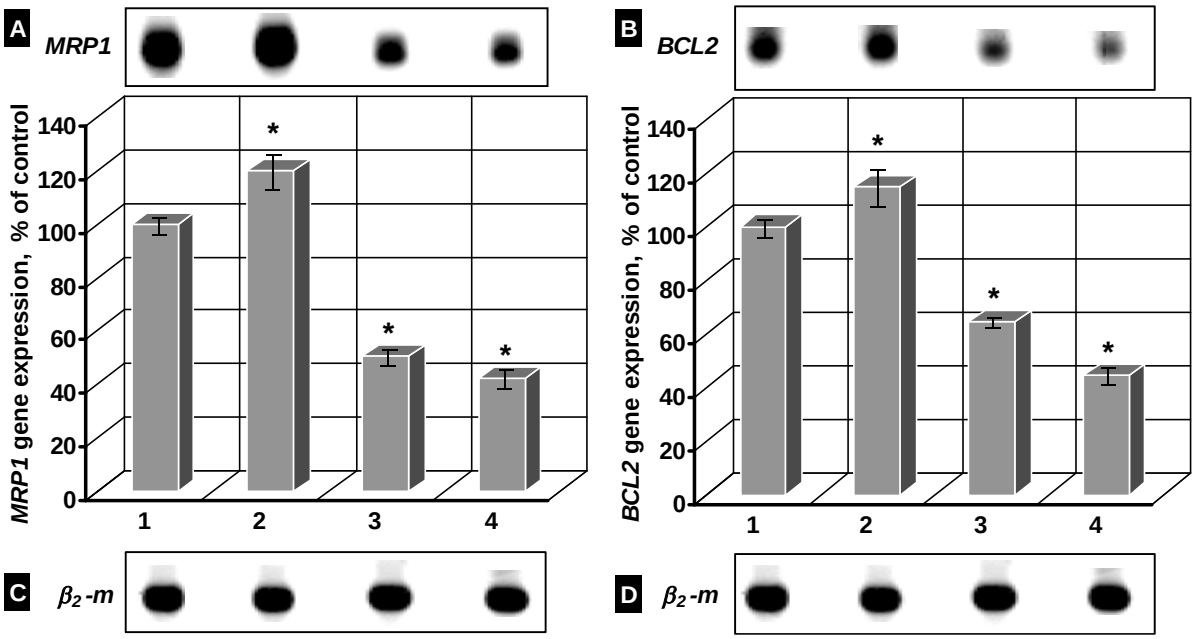

Figure 9. Representative images of RT-PCR products of MRP1 (A), BCL2 (B) and β_2-m (C and D, internal standard) mRNA and densitometric analysis of bands in A549 lung cancer cells incubated with following formulations: (1) Control (medium); (2) mixture of LHRH-PEG-DOX-MSN and LHRH-PEG-CIS-MSN; (3) mixture of LHRH-PEG-siRNA(BCL2)-DOX-MSN, LHRH-PEG-siRNA(MRP1)-DOX-MSN, LHRH-PEG-siRNA(BCL2)-CIS-MSN and LHRH-PEG-siRNA(MRP1)-CIS-MSN; and (4) Mixture of LHRH-PEG-siRNA(BCL2)-MSN and LHRH-PEG-siRNA(MRP1)-MSN. Gene expression in control was set to 100%. Means ± SD are shown. *$P < 0.05$ when compared with control.

Task 3. To select and characterize an optimal regimen of aerosol generation, nebulizer performance, droplet size and dose, dynamic stability of MSN based DDS and body distribution of airborne nanoparticles *in vivo* (months 6-12):

A Collison nebulizer (BGI) connected to four-port, nose-only exposure chambers (CH Technologies) was used for inhalation co-delivery of drugs and siRNA by MSN based DDS (Fig. 10). The solution of DDS was aerosolized at a flow rate of 2 L/min and then diluted by an additional 2 L/min air. The flow meter allows regulating drug concentration and air flow.

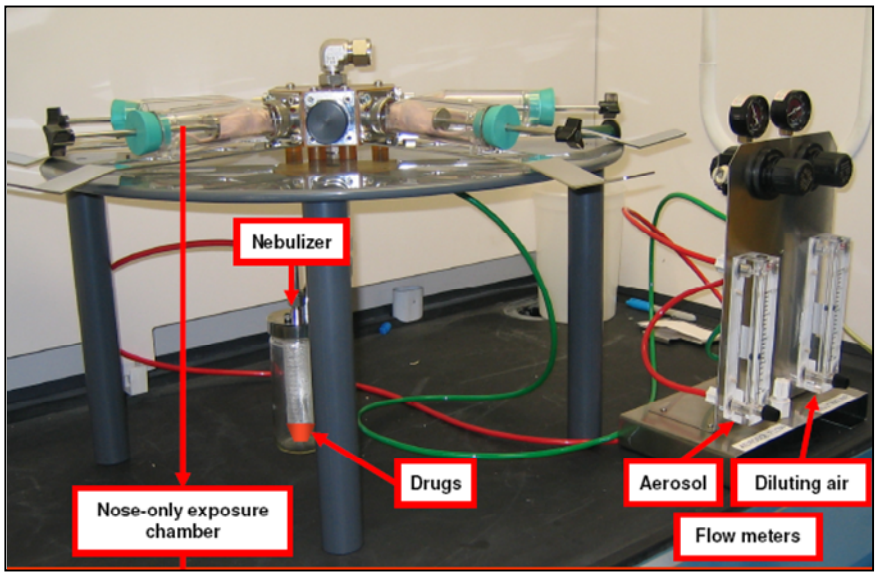

Figure 10. Installation for inhalation treatment.

3a. *Testing of DDS stability after aerolization (months 6-7)*

Pneumatic aerosol nebulizers, such as Collison nebulizer used in this study, are known to exert considerable shear forces on the particles being generated. In addition, the liquid in the devise is constantly re-circulated which could lead to the accumulation of the stress during the prolonged nebulization. In certain cases the stress can lead to the loss of particle integrity. Thus, to ensure that the integrity of the DDS is not affected during exposure experiments, the Collison nebulizer was operated continuously for 60 min at a low pressure of 20 psi and size distributions of airborne and liquid-borne MSN were examined before and after nebulization. The airborne size of LHRH-PEG-siRNA-Drug-MSN was monitored every 15 min using a Scanning Mobility Particle Sizer (SMPS) (model 3936, TSI Inc., Shoreview, MN). The size of the liquid-borne DDS was analyzed using photon correlation spectroscopy (PCS) using a Malvern Nano ZS90 (Malvern Instruments, UK). SPMS measurements demonstrated that the airborne particle diameter is ~160 nm and did not vary substantially over aerosolization time. At the same time, PCS measurements represented that the particles diameter in liquid is ~180 nm (Fig. 2C). The small discrepancy in airborne and liquid-borne sizes of DDS could be related to the fact that different methods were employed for the size measurements. Thus SMPS determines particle electrical mobility, while PCS determines hydrodynamic particle diameter. Overall, SPMS and PCS measurements do not show a significant change in airborne and liquid-borne size of MSN based DDS which indicates

that the LHRH-PEG-siRNA-Drug-MSN were not substantially damaged during their continuous aerosolization.

3b. *Developing of in vivo aerolization procedure (months 7-8)*

In addition, the drug delivery and exposure system itself was characterized to estimate the inhaled dose and to ensure that all test animals received a similar dose of the DDS. In order to test the mass distributions across the ports of inhalation system, DDS labeled with Cy.5.5 dye were used in this study. Here, a probe was inserted into each containment tube so that a probe's inlet would be in approximately the same position as an animal's nose. The air flow of 25 mL/min through each probe was provided by a pump with a low-flow adapter, and the particles were collected on a filter positioned immediately after a containment tube. The sampling airflow was selected to mimic mouse breathing. The four probes at ports P1, P2, P4, and P5 were operated simultaneously. The concentration of Cy5.5 labeled DDS was 1mg/mL and aerosolization time was 10 min. The mass of Cy5.5 labeled DDS collected on each filter was quantified by a fluorometer (FM109515, Sequoia-Turner Corp., Mountain View, CA) using previously obtained calibration curve. Briefly, each filter with collected particles was soaked in ethanol in a glass container for 4 hours to dissolve the Cy5.5-DDS and then an aliquot of 100 µL was used to measure fluorescence intensity from each sample. As could be seen in Figure 11, the relative mass fraction did not vary substantially across four exposure ports.

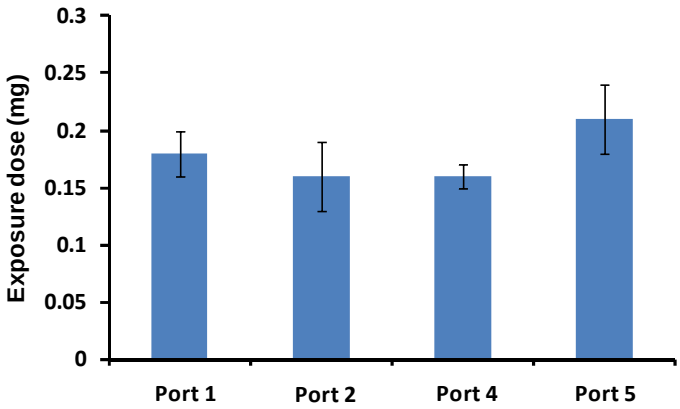

Figure 11. The DDS mass distributions across the ports of inhalation system. Aerosolization time-10 min. LHRH-PEG-siRNA-Drug-MSN concentration – 1 mg/mL.

Based on the obtained DDS mass distribution measurements, the doses of the inhaled drugs required for the planed *in vivo* studies were adjusted by changing initial concentrations of LHRH-PEG-siRNA-Drug-MSN complexes.

3c. *Evaluation of MTD of the prepared DDS on mice (months: 8-10)*

In vivo toxicity of drug-loaded formulations: (1) LHRH-PEG-siRNA-DOX-MSN (2) LHRH-PEG-siRNA-CIS-MSN and (3) 1:1 mixture of LHRH-PEG-siRNA-DOX-MSN and LHRH-PEG-siRNA-CIS-MSN was evaluated to determine maximum tolerated dose (MTD). The MTD was defined as the allowance of a median body weigh loss of 15% of the control and causes neither

death due to toxic effects nor remarkable changes in the general signs within 3 days after treatments. Six different drug doses were used in our studies: (1) control- 0 mg/kg (mg of drug per 1 kg of mouse body weight); (2) 1 mg/kg; (3) 2 mg/kg; (4) 3 mg/kg; (5) 4 mg/kg; and (6) 5 mg/kg; The selection of drug doses was based on the previous study, which demonstrated that MTD of free DOX is 2.5 mg/kg[13-14]. In each instance, the present studies included 18 experimental groups consisting of 5 nu/nu nude mice, which were exposed to single inhalation of either (1) LHRH-PEG-siRNA-DOX-MSN; or (2) LHRH-PEG-siRNA-CIS-MSN or (3) 1:1 mixture of LHRH-PEG-siRNA-DOX-MSN at the above mentioned concentrations. The weight of mice in control and treated groups were recorded during 3 days after single inhalation. All procedures used were according to the guidelines of the Care and Use of Laboratory Animals and were approved by the Animal Care Committee of the Rutgers University and USAMRMC Animal Care and Use Review Office (ACURO). According to Figure 12, none of the concentrations used in this study was toxic to the mice. The obtained result demonstrated the advantage of using the developed MSN based DDS in comparison to the free drug.

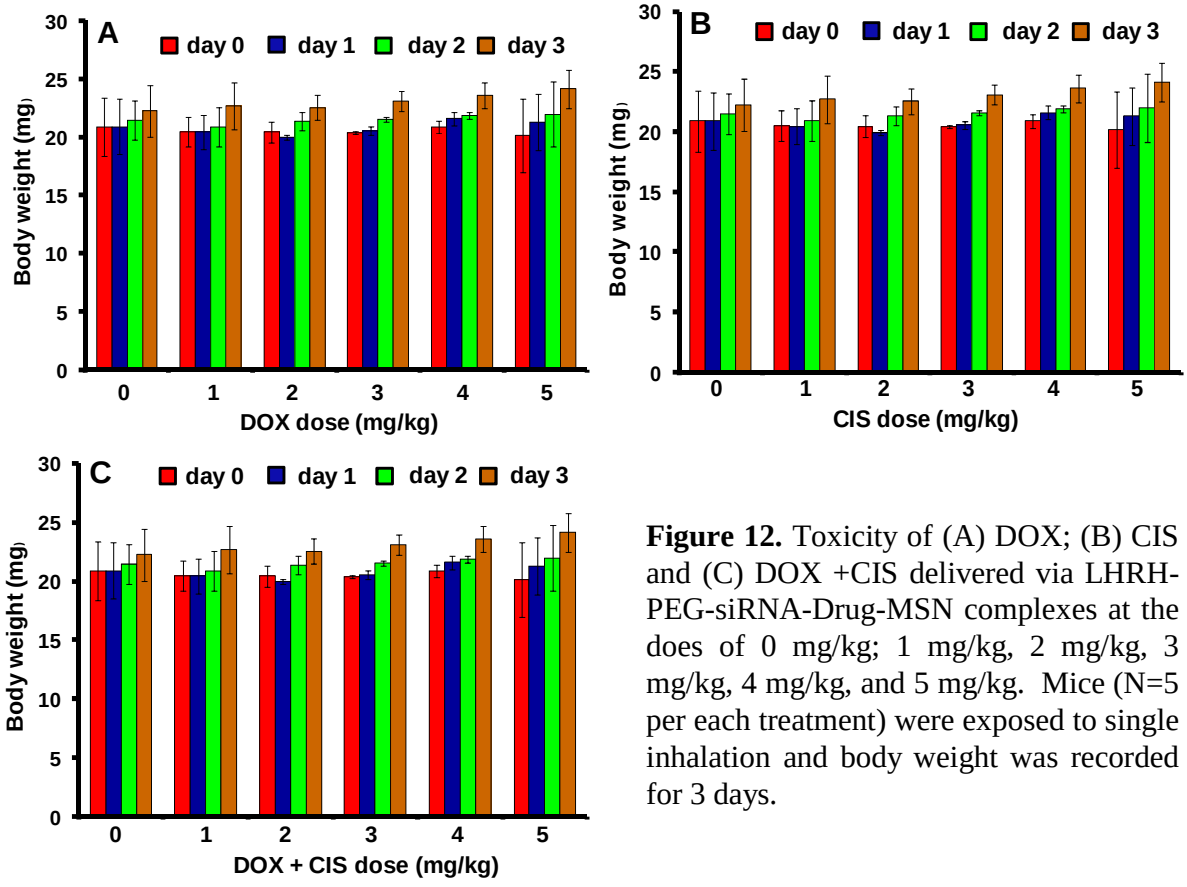

Figure 12. Toxicity of (A) DOX; (B) CIS and (C) DOX +CIS delivered via LHRH-PEG-siRNA-Drug-MSN complexes at the does of 0 mg/kg; 1 mg/kg, 2 mg/kg, 3 mg/kg, 4 mg/kg, and 5 mg/kg. Mice (N=5 per each treatment) were exposed to single inhalation and body weight was recorded for 3 days.

3d. *Preparation of mice with lung tumor (months 8-9)*

Six week old NCR nude mice (20 g) were purchased from Taconic Farms, Inc. (Germantown, NY). A mouse orthotopic model of human lung cancer developed in our lab was used[2]. Briefly, A549 human lung adenocarcinoma epithelial cells transfected with luciferase ($5–8 \times 10^6$) were resuspended in 0.1 mL of RPMI medium containing 20% FBS, mixed with 5 μM EDTA and

administered intratracheally to the murine lung of 10 mice through a catheter (Fig. 13A). It was shown that a slight disruption of the pulmonary epithelium or the surfactant layer by co-administration of either pancreatic elastase or EDTA allowed significantly better tumour engraftment[15]. At the same time, cancer cell suspensions tolerate this concentration of EDTA, and animals subjected to EDTA at this concentration exhibit no histological pulmonary abnormalities. The progression of tumour growth was monitored by an IVIS (Xenogen, Alameda, CA) imaging system (Fig. 13C). Rapid growth of lung tumor developed in 90% of animals (total 9 mice).

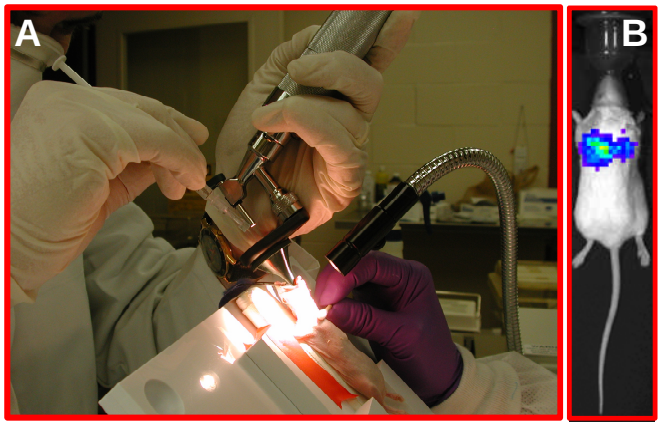

Figure 13. Orthotopic lung model. (A) Human A549 lung cancer cells transfected with luciferase were intratracheally injected into the lungs of nude mice. (B) Typical bioluminescent image of a mouse with lung tumor 4 weeks after instillation of cancer cells. Intensity of bioluminescence is expressed by different colors, with blue reflecting the lowest intensity and red indicating the highest intensity.

3e. *Evaluation of DDS accumulation in living mice (months 9-10)*

For an efficient lung cancer treatment, the active ingredients of DDS should be easily delivered by inhalation to the lung cancer cells and retained there. Four weeks after the instillation of tumor cells, 9 mice, which developed lung tumors, were exposed to the single inhalation of LHRH-PEG-siRNA-DOX-MSN. The dose of all formulations containing doxorubicin for inhalation administration was 2.5 mg/kg for the single injection. The distribution of labeled MSN (Cy5.5, near infrared dye), siRNA (FAM, green dye) and DOX (red, intrinsic fluorescence) was analyzed in live anesthetized animals at different time points after injection using IVIS Xenogen imaging system (Fig. 14A and 14B). As Figure 14 demonstrates, a strong fluorescence background from blood and tissues of the mice complicated an evaluation of DDS organ distribution in the live animals.

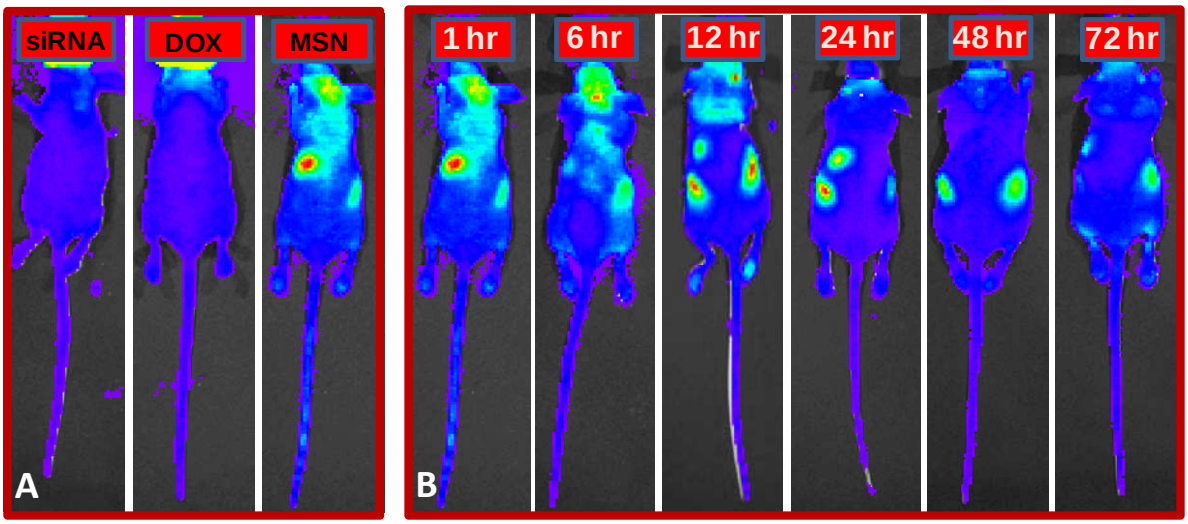

Figure 14. (A) Distribution of FAM-siRNA, DOX and Cy5.5-MSN after 1 hr following mice exposure to single inhalation with LHRH-PEG-siRNA-DOX-MSN complexes. (B) Distribution of Cy5.5 labeled MSN at different time points (1hr, 6hr, 12hr, 24hr, 48hr, 72hr) after mice exposure to single inhalation with LHRH-PEG-siRNA-DOX-MSN complexes. The intensity of fluorescence was represented on composite light/fluorescent images by different colors with blue color reflecting the lowest fluorescence and red color – the highest intensity.

3f. *Evaluation of DDS accumulation in mice organs (months 9-10)*

After measuring the fluorescence distribution in the entire animal, four mice were sacrificed after 3 hr and five mice after 72 hr. Furthermore, organs were excised and distribution of FAM-siRNA, DOX and Cy5.5-labeled DDS was studied using the IVIS system. (Fig. 15A and 15B). The data show that inhalation delivery substantially enhanced lung exposure to DDS and limited the accumulation of DDS in other organs. Moreover, pulmonary delivery sufficiently enhances the accumulation of DDS in the cancer tumor. Thus, the total amount of DDS retained in the lungs within 3 hr after inhalation was 73%. While the amount of MSN based DDS after single inhalation in liver, kidneys and spleen was 17%, 9% and 1%, respectively. Similar profiles of organ distribution were found also for siRNA and DOX (Fig. 15A). Sufficient amount of LHRH-PEG-siRNA-DOX-MSN nanoparticles retained in the cancer tumor after 72 hr, while the rest of the complexes were cleared from lungs and accumulated in the liver and kidneys (Fig. 15B).

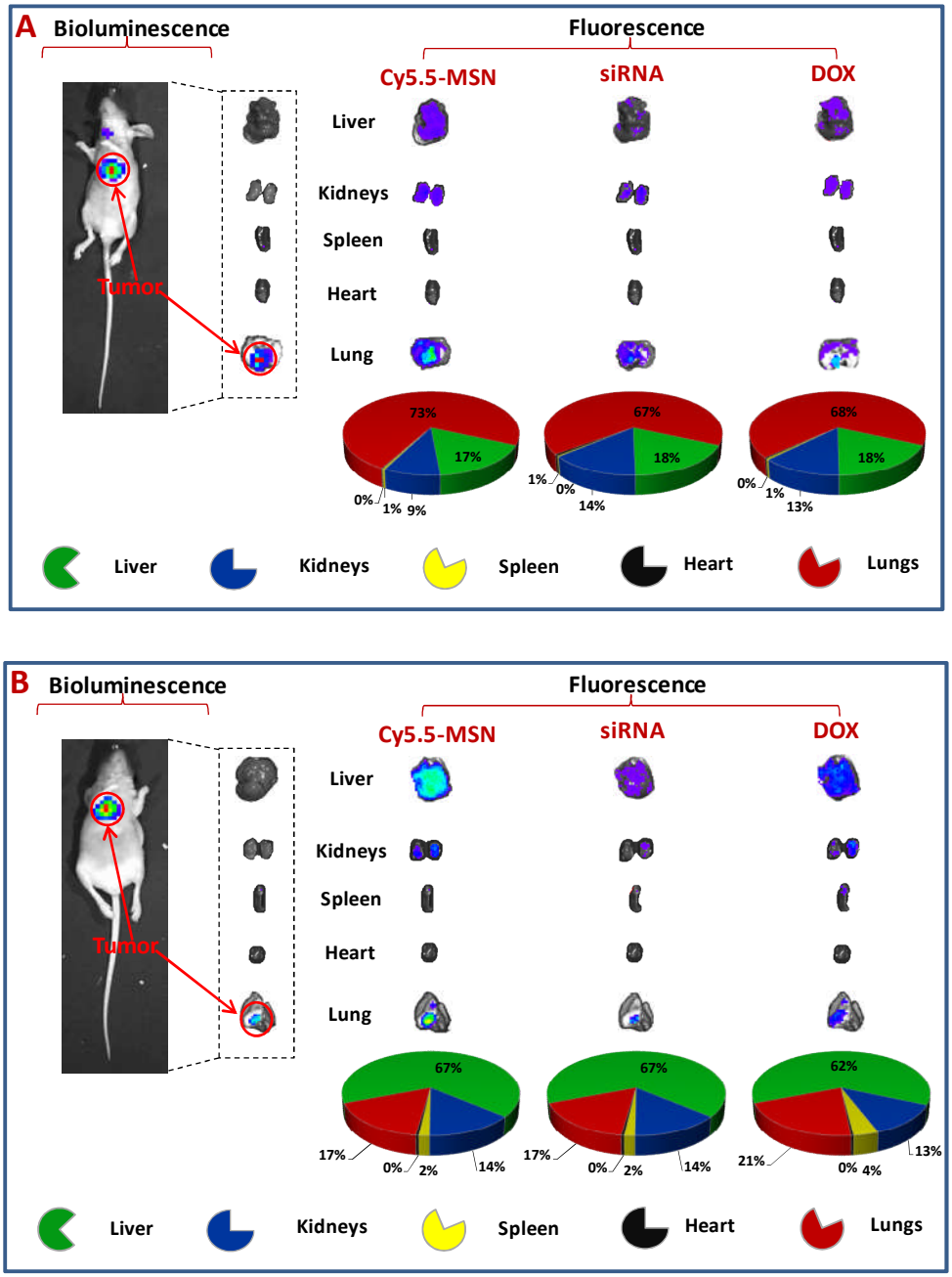

Figure 15. Organ and tumor content of LHRH-PEG-siRNA-DOX-MSN. MSN and siRNA were labeled with near infrared Cy5.5 dye and FAM (green) respectively. Intrinsic fluorescence of DOX (red) was employed. LHRH-PEG-siRNA-DOX-MSN nanoparticles were injected into the mice by inhalation. The distribution of Cy5.5-MSN, FAM-siRNA and DOX was analyzed in different organs (A) 3 hr and (B) 72 hr after injection using IVIS Xenogen imaging system. The intensity of bioluminescence (tumor cells) and fluorescence (MSN, siRNA and DOX) are expressed by different colors with blue color reflecting the lowest intensity and red color reflecting the highest intensity.

3g. *Estimation of adverse side effects for treatment (months 10-12)*

In order to estimate adverse side of treatment, the different organs (liver, kidneys, spleen, heart, brain and lungs) were isolated from mice on the 3rd day after their exposure to single inhalation with 1:1 mixture of LHRH-PEG-siRNA-DOX-MSN and LHRH-PEG-siRNA-CIS-MSN (drug concentration – 5mg/kg). Tissues were fixed with in 10% phosphate-buffered formalin. Samples were subsequently dehydrated and embedded in Paraplast. Sections (5 μm) were cut, stained with hematoxylin-eosin and imaged using Olympus (Melville, NY) microscope. According to histopathologic analysis (Fig. 16), the signs of damage were not observed in healthy organs after the mice treatment with 1:1 mixture of LHRH-PEG-siRNA-DOX-MSN and LHRH-PEG-siRNA-CIS-MSN (drug concentration – 5mg/kg).

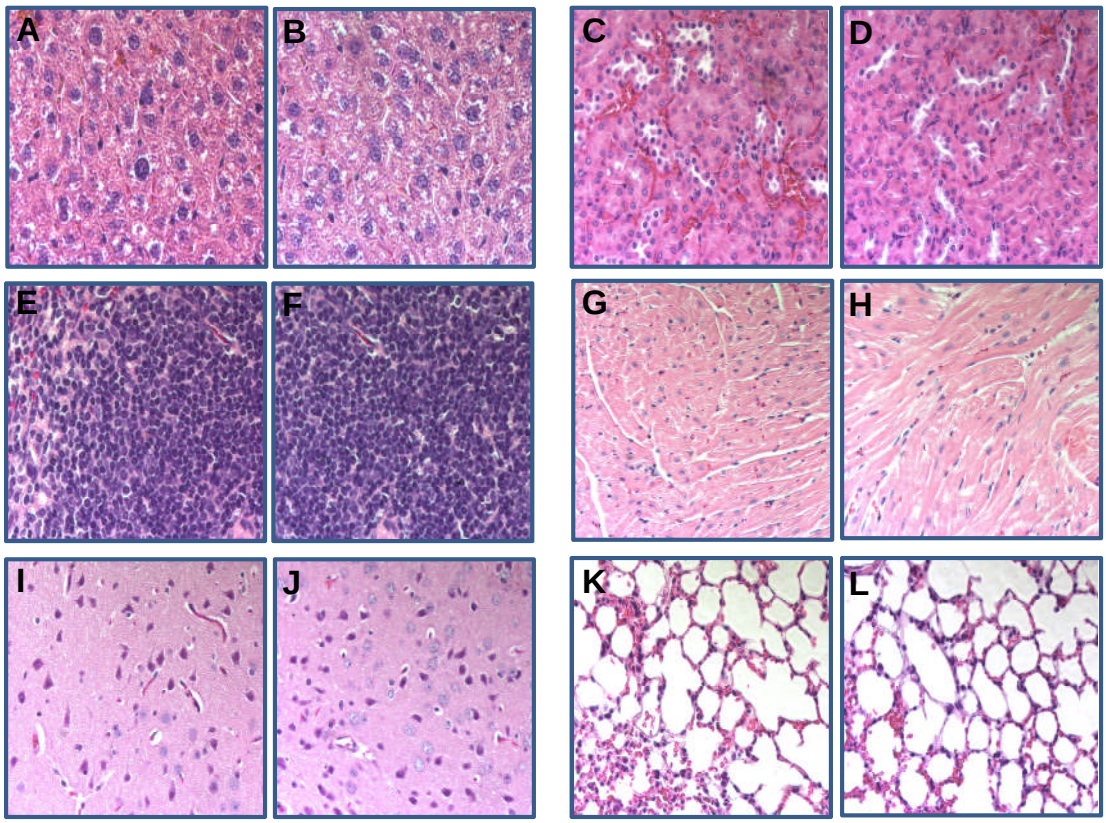

Figure 16. Histologic sections of (A-B) liver, (C-D) kidneys, (E-F) spleen, (G-H) heart, (I-J) brain and (K-L) lungs without treatment and after mice exposure to single inhalation with 1:1 mixture of LHRH-PEG-siRNA-DOX-MSN and LHRH-PEG-siRNA-CIS-MSN (drug concentration – 5mg/kg).

Key Research Accomplishments

- The tumor targeted nanomedicine platform based on MSNs has been developed for inhalation local delivery of anticancer drugs such as Doxorubicin and Cisplatin as cell death inducers in combination with MRP1 and BCL2 targeted siRNAs as suppressors of cellular resistance, respectively.
- The developed DDS system is capable of effectively delivering inside cancer cells anticancer drugs (doxorubicin and cisplatin) combined with two types of siRNA targeted to MRP1 and BCL2 mRNA.
- Suppression of cellular resistance by siRNA effectively delivered inside cancer cells with the developed DDS substantially enhanced the cytotoxicity of anticancer drugs.
- Local delivery of DDS by inhalation and specific targeting to lung cancer cells led to the preferential accumulation of drugs and siRNA in the mouse lungs prevented their escape into the systemic circulation, and limited adverse side effect in healthy organs.

Reportable Outcome

- **Manuscript:** submitted to *Journal of Drug Targeting* (appendix A).
- **Presentations:** The PI (Oleh Taratula) was invited to present the current work at ACS 42nd Middle Atlantic Regional Meeting; Section: Medicinal Chemistry and Chemical Biology of Anticancer Agents (appendix B).
- **Published abstract:** Oleh Taratula, Olga Garbuzenko, Alex M. Chen, Zuocheng Wang, Gediminas Mainelis and Tamara Minko. Oral presentation: "Innovative Strategy for Treatment of Lung Cancer: Inhalatory Co-Delivery of Anticancer Drugs and siRNA for Suppression of Cellular Resistance". ACS 42nd Middle Atlantic Regional Meeting: International Year of Chemistry at the University of Maryland, College Park, Maryland, May 21-24, 2011 (appendix C).

Manuscript submitted to *Journal of Drug Targeting is presented as* appendix A.

The Symposium Program Highlights which shows the name of the PI, the title and abstract of his talk is provided as an appendices B and C.

Conclusions

The experimental data confirm that the developed DDS for pulmonary drug administration satisfies the major prerequisites for effective treatment of non-small cell lung carcinoma. Therefore, the proposed cancer targeted MSN-based system for complex delivery of drugs and siRNA has high potential in the effective treatment of lung cancer. Based on the successful outcome of the current project, PI is planning to apply for a new grant in order to perform a detailed study of lung cancer treatment with the developed DDS.

References

1. Jaracz, S., Chen, J., Kuznetsova, L.V. & Ojima, L. Recent advances in tumor-targeting anticancer drug conjugates. *Bioorgan Med Chem* **13**, 5043-5054 (2005).
2. Garbuzenko, O.B., *et al.* Inhibition of lung tumor growth by complex pulmonary delivery of drugs with oligonucleotides as suppressors of cellular resistance. *P Natl Acad Sci USA* **107**, 10737-10742 (2010).
3. Chen, A.M., *et al.* Co-delivery of doxorubicin and Bcl-2 siRNA by mesoporous silica nanoparticles enhances the efficacy of chemotherapy in multidrug-resistant cancer cells. *Small* **5**, 2673-2677 (2009).
4. Perry, C.C. An overview of silica in biology: its chemistry and recent technological advances. *Prog Mol Subcell Biol* **47**, 295-313 (2009).
5. Bravo-Osuna, I., Teutonico D, Arpicco S, Vauthier C, Ponchel G. Characterization of chitosan thiolation and application to thiol quantification onto nanoparticle surface. *Int J Pharm* **340**, 173-182 (2007).
6. Muggia, F.M., *et al.* Phase I/II study of intraperitoneal floxuridine and platinums (cisplatin and/or carboplatin). *Gynecol Oncol* **66**, 290-294 (1997).
7. Gu, J., Su S, Li Y, He Q, Zhong J, Shi J. Surface modification−complexation strategy for cisplatin loading in mesoporous nanoparticles. *J Phys Chem Lett* **1**, 3446–3450 (2010).
8. Taylor, A., Krupskaya Y, Krämer K, Füssel S, Klingeler R, Büchner B, Wirth MP. Cisplatin-loaded carbon-encapsulated iron nanoparticles and their in vitro effects in magnetic fluid hyperthermia. *Carbon* **48**, 2327-2334 (2010).
9. Dharap, S.S. & Minko, T. Targeted proapoptotic LHRH-BH3 peptide. *Pharmaceut Res* **20**, 889-896 (2003).
10. Taratula, O., *et al.* Surface-engineered targeted PPI dendrimer for efficient intracellular and intratumoral siRNA delivery. *J Control Release* **140**, 284-293 (2009).
11. Saad, M., Garbuzenko OB, Minko T. Co-delivery of siRNA and an anticancer drug for treatment of multidrug-resistant cancer. *Nanomedicine (Lond)* **3**, 761-776 (2008).
12. Anderson, M.E. Glutathione: an overview of biosynthesis and modulation. *Chem Biol Interact* **112**, 1-14 (1998).
13. Dharap, S.S., *et al.* Tumor-specific targeting of an anticancer drug delivery system by LHRH peptide. *P Natl Acad Sci USA* **102**, 12962-12967 (2005).

14. Minko, T., Kopeckova, P. & Kopecek, J. Efficacy of the chemotherapeutic action of HPMA copolymer-bound doxorubicin in a solid tumor model of ovarian carcinoma. *Int J Cancer* **86**, 108-117 (2000).
15. March, T.H., Marron-Terada PG, Belinsky SA. Refinement of an orthotopic lung cancer model in the nude rat. *Vet Pathol* **38**, 483-490 (2001).

List of personnel receiving pay from the research effort:

1. Oleh Taratula, principal investigator
2. Min Zhang, co-investigator

Appendices

Appendix A: Manuscript submitted to *Journal of Drug Targeting*

Appendix B: ACS 42nd Middle Atlantic Regional Meeting (2011) program highlights.

Appendix C: Published abstract: Oleh Taratula, Olga Garbuzenko, Alex M. Chen, Zuocheng Wang, Gediminas Mainelis and Tamara Minko. Oral presentation: "Innovative Strategy for Treatment of Lung Cancer: Inhalatory Co-Delivery of Anticancer Drugs and siRNA for Suppression of Cellular Resistance". ACS 42nd Middle Atlantic Regional Meeting: International Year of Chemistry at the University of Maryland, College Park, Maryland, May 21-24, 2011.

Appendix A

Innovative strategy for treatment of lung cancer: targeted nanotechnology-based inhalation co-delivery of anticancer drugs and siRNA

OLEH TARATULA*, OLGA B. GARBUZENKO, ALEX M. CHEN AND TAMARA MINKO*

Department of Pharmaceutics, Ernest Mario School of Pharmacy, Rutgers, The State University of New Jersey, Piscataway, NJ 08854

***Corresponding authors:**
Tamara Minko, Ph.D.
Professor II and Chair
Department of Pharmaceutics
Ernest Mario School of Pharmacy
Rutgers, The State University of New Jersey
160 Frelinghuysen Road
Piscataway, NJ 08854–8020
Phone: 732-445-3831 x 214
Fax: 732-445-3134
Email: minko@rci.rutgers.edu
http://www.rci.rutgers.edu/~ceutics/minkohome.shtml

Oleh Taratula, Ph.D.
Research Associate
Department of Pharmaceutics
Ernest Mario School of Pharmacy
Rutgers, The State University of New Jersey
160 Frelinghuysen Road
Piscataway, NJ 08854–8020
Phone: 732-445-3831 x 214
Fax: 732-445-3134
Email: oleht@pegasus.rutgers.edu

Keywords:

Mesoporous silica nanoparticles; pulmonary delivery; siRNA; doxorubicin; cisplatin; lung cancer, LHRH peptide; body distribution; drug resistance.

Abstract

A tumour targeted mesoporous silica nanoparticles (MSN)-based drug delivery system (DDS) was developed for inhalation treatment of lung cancer. The system was capable of effectively delivering inside cancer cells anticancer drugs (doxorubicin and cisplatin) combined with two types of siRNA targeted to MRP1 and BCL2 mRNA for suppression of pump and nonpump cellular resistance in non-small cell lung carcinoma, respectively. Targeting of MSN to cancer cells was achieved by the conjugation of LHRH peptide on the surface of MSN via poly(ethylene glycol) spacer. The delivered anticancer drugs and siRNA preserved their specific activity leading to the cell death induction and inhibition of targeted mRNA. Suppression of cellular resistance by siRNA effectively delivered inside cancer cells and substantially enhanced the cytotoxicity of anticancer drugs. Local delivery of MSN by inhalation led to the preferential accumulation of nanoparticles in the mouse lungs, prevented the escape of MSN into the systemic circulation, and limited their accumulation in other organs. The experimental data confirm that the developed DDS satisfies the major prerequisites for effective treatment of non-small cell lung carcinoma. Therefore, the proposed cancer targeted MSN-based system for complex delivery of drugs and siRNA has high potential in the effective treatment of lung cancer.

Introduction

Lung cancer is a leading cause of cancer death in both men and women (Molina et al. 2008). Only about 14% of the patients with lung cancer survive for five years, and the majority die within two years (Minna 2008; Youlden et al. 2008). One of the main reasons for the poor survival rates among patients with lung cancer is the limited efficiency of traditional treatment. Since lung cancer is often widely disseminated among the lung tissues, spread out tumours are not easy to remove by surgery and therefore, chemotherapy and/or radiotherapy is the only treatment of choice. The conventional parenteral systemic chemotherapy uses high doses of toxic anticancer drugs which often produce severe adverse side effects on healthy organs (Jaracz et al. 2005; Reference 2007). Therefore, an ideal anticancer therapy would involve the local administration of high drug concentration directly to the target tissue for the maximum treatment effect, limitation of drug degradation in the systemic circulation, and low adverse side effects. For lung diseases, pulmonary drug delivery approach had been developed to satisfy this requirement (Melani 2007). Inhalation route of drug administration has several advantages over systemic delivery routes. The most important advantage of an inhalatory route for drug administration is that lungs provide a large absorptive surface for aerosol deposition and allow the drug to avoid the first-pass metabolic degradation (Yu 1997; Koshkina et al. 2001). Despite these advantages, the efficient nebulization and inhalation delivery is possible only for a limited number of drugs. Therefore, a special drug delivery system (DDS) is required for inhalation deposition of chemotherapeutic agents into the lungs (Koshkina et al. 2001). Recent reports demonstrated a development of some DDS based on liposomes and polymer nanoparticles for pulmonary delivery of variety anticancer drugs (Koshkina et al. 2001; Garbuzenko et al. 2009;

Garbuzenko et al. 2010); (Borm and Kreyling 2004; Nguyen 2008; Beck-Broichsitter et al. 2009). It was shown that pulmonary delivery improves retention of active agents in the lungs and limits their penetration into the blood circulation (Valle et al. 2007; Valle 2008; Garbuzenko et al. 2009) creating prerequisites for limiting adverse side effects of chemotherapy.

The efficacy of chemotherapy is also limited by intrinsic or the rapidly developed tumour resistance. The main mechanisms of this resistance are common to most cancers and include “pump” and “nonpump” resistance (Pakunlu et al. 2003; Minko et al. 2004; Pakunlu et al. 2004). The pump resistance is caused by membrane transporters that pump out the anticancer agents from cells, decreasing the efficacy of the treatment. Inhibition of pump resistance augments intracellular drug concentrations without increasing the total applied drug dose. However, even if drug efflux pumps are suppressed, cells still can survive high intracellular drugs concentrations due to the activation of nonpump resistance. One of the main mechanisms of nonpump resistance is the activation of cellular antiapoptotic defence. Consequently, only simultaneous suppression of both types of cell resistances is capable of substantially increasing the efficacy of anticancer drugs (Pakunlu et al. 2006; Garbuzenko et al. 2010).

Recently, we developed a liposome-based system for pulmonary co-delivery of anticancer drugs and antisense oligonucleotides as the suppressors of both pump and nonpump cellular resistance (Garbuzenko et al. 2010). The simultaneous delivery of anticancer drug(s) and suppressors of pump and nonpump resistance via the inhalation route demonstrated enhanced antitumor activity and lower adverse side effects of treatment on healthy organs. It should also be mentioned that severe adverse side effects of chemotherapy can be further (in addition to the local inhalatory delivery) limited by developing targeted tumour-specific DDS (Saad et al. 2008;

Taratula et al. 2009; Savla et al. 2011). We demonstrated that modification of DDS with cancer targeting ligand such as LHRH peptide, which receptors overexpressed in the plasma membrane of cancer cells, can facilitate delivery of therapeutic agents specific to the human lung cancer cells and limit adverse side effects of the treatment (Saad et al. 2008; Savla et al. 2011).

Lately, the application of mesoporous silica nanoparticles (MSN) as carriers for the targeted DDS has been investigated (Radu et al. 2004; Chen et al. 2009; Tao et al. 2010). Large pore volume and surface area of MSN make them an ideal platform for loading a large amount of drugs inside the pores and conjugation of other active components (e.g. siRNA) on the surface for simultaneous delivery into cells. Furthermore, MSN exhibit biocompatibility at concentrations tolerable for pharmacological applications (Vivero-Escoto et al. 2010). It was reported that PEG modified MSN has good blood compatibility as they demonstrated minimized nonspecific binding to human serum proteins and the phagocytosis by macrophages (He et al. 2010). Due to biocompatibility and the possibility of lodging different drug molecules, MSN have been widely employed as cell markers (Lin et al. 2005), drug and gene delivery vehicles, (Radu et al. 2004; Chen et al. 2009; Tao et al. 2010) and enzyme carriers (Slowing et al. 2007). Moreover, our previous report demonstrated that mesoporous silica nanoparticles can be efficiently employed for co-delivery of doxorubicin (DOX) and a siRNA. The anticancer efficacy of DOX delivered by DDS that contains siRNA in addition to drugs was 132 times higher when compared with the same concentration of free DOX, mainly because the siRNA used suppressed cellular resistance and, as a result, provided for better killing of cells by the anticancer drug (Chen et al. 2009).

The present work is aimed at developing a lung tumour targeted DDS for inhalation therapy of lung cancer that contains five main components: (1) MSN as a carrier; (2) anticancer drugs; (3) suppressor of pump drug resistance; (4) suppressor of nonpump cellular resistance (5) targeting moiety specific for lung cancer cells. To the best of our knowledge, this is the first report, which demonstrates an application of MSN as nanocarriers for tumour specific targeted co-delivery of chemotherapeutic agents and suppressor of cancer cell resistance via the pulmonary route.

Material and methods

Materials

N-Cetyltrimethylammonium bromide (CTAB), (3-Mercaptopropyl)trimethoxysilane (MPTS), Aldrithiol-2, sodium hydroxide, Tetraethoxysilane (TEOS), 4-(Dimethylamino) pyridine (DMAP), triethylamine, 1-Ethyl-3-(3-dimethyllaminopropyl)carbodiimide hydrochloride (EDC·HCl), methanol, toluene, Dimethyl sulfoxide (DMSO), Dimethylformamide (DMF), Dichloromethane (DCM), HCl, glacial acetic acid, 5,5'-dithiobis-(2-nitrobenzoic acid) (Ellman's reagent), o-phenylenediamine (OPDA) were obtained from Sigma Chemical Co. (St. Louis, MO) and used without further purification. Glutathione Reduced was purchased from AMRESCO (Solon, OH). Reductacryl was obtained from EMD Chemicals, Inc. (Gibbstown, NJ) and HS-PEG-COOH from Rapp Polymere GmbH (Tuebingen, Germany). Cy5.5 NHS ester was purchased form GH Healthcare Life Sciences (Piscataway, NJ). Synthetic analog of Luteinizing Hormone-Releasing Hormone (LHRH) decapeptide (Gln-His-Trp-Ser-Tyr-DLys(D-Cys)-Leu-Arg-Pro) was synthesized according to our design by American Peptide Company, Inc.

(Sunnyvale, CA). DOX and cisplatin (CIS) were obtained from Sigma Chemical Co. (St. Louis, MO). siRNA was custom synthesized by Invitrogen (Carlsbad, CA). The sequences of the siRNA targeted to BCL2 mRNA were: 5'-[S-S-C6]-GUG-AAG-UCA-ACA-UGC-CUG-CdTdT-3' (sense strand) and 5'-GCA-GGC-AUG-UUG-ACU-UCA-CdTdT-3' (antisense strand). The sequence of the siRNA targeted to MRP1 mRNA was: 5'-[S-S-C6]-GGC-UAC-AUU-CAG-AUG-ACA-CdTdT-3' (sense strand) and 5'-GUG-UCA-UCU-GAA-UGU-AGC-CdTdT-3'. In order to visualize siRNA with fluorescence microscope, antisense strand was additionally modified with fluorescent dye 5'-tetramethylrhodamine (TAMRA): 5'-TAMRA-GCA-GGC-AUG-UUG-ACU-UCA-CdTdT-3'.

Methods

Synthesis of mesoporous silica nanoparticles. Mobile Crystaline Material-41 (MCM-41) type of MSN was synthesized by using a surfactant-templated, base-catalyzed condensation method as previously reported (Chen et al. 2009; Slowing 2009). 0.5 g of CTAB was dissolved in 240 mL of deionized (DI) water and then mixed with 1.75 mL of aqueous sodium hydroxide solution (2 M) in a 500 mL round bottom flask. The temperature of the mixture was adjusted to 353 °K and 2.5 mL of TEOS was added drop wise to the flask under vigorous stirring. The reaction was allowed to proceed for 2 h to give white precipitate. The resulting product was filtered, washed with DI water and methanol, and then dried at 60 °C under high vacuum to yield the as-synthesized MSN. To remove the surfactant template (CTAB), the as-synthesized MSN were refluxed for 17 h in a mixture of 1.5 mL of HCl (37.4 wt%) and 150 mL of methanol. The resulting material was filtered and extensively washed with DI H_2O and methanol. The

surfactant-free MSN were then dried under high vacuum at 60 °C overnight to remove the remaining solvent from the particles.

Synthesis of 3-mercaptopropyl-functionalized MSN (MPTS-MSN). 0.4 mL of MPTS were added to 50 mL of anhydrous toluene in a flask. Then 400 mg of surfactant-free MSN were added. After 24 h refluxing, the heating was stopped and the vessel was left to cool down to ~ 35 °C. The resulting powder suspension was then centrifuged at 10 000 rpm for 20 min to remove the free MPTS and toluene. Then, the precipitate was rinsed with toluene and anhydrous methanol. Thus-obtained powder was dried under vacuum at 75 °C overnight to remove any remaining solvent.

Synthesis of pyridylthiol-terminated MSN. In order to prepare pyridylthiol-terminated nanoparticles, 250 mg of MPTS-MSN in 25 mL of methanol were added drop wise to a solution containing 0.55 g of Aldrithiol-2, 0.2 mL of glacial acetic acid, and 10 mL of methanol. After the reaction within 24 h at room temperature, the mixture was centrifuged at 10 000 rpm for 20 min to purify pyridylthiol-terminated MSN. Then, the precipitate was rinsed with methanol and dried under vacuum at 75 °C overnight to remove any remaining solvent. The thiol groups on the surface of 3-mercaptopropyl-functionalized MSN before and after reaction with Aldrithiol-2 were quantified by using Ellman's reagent (Bravo-Osuna 2007).

Loading of DOX and CIS inside the pores of pyridylthiol-terminated MSN. DOX loaded MSN nanoparticles were prepared according to the previously described procedure (Chen et al. 2009). 5.0 mg of pyridylthiol-terminated MSN were added into 5 mL of DOX solution in 3:5 (v:v) MeOH:H_2O cosolvent (4.5 mg/mL) and sonicated for 5 min to obtain a well-dispersed

suspension. This suspension was then stirred at room temperature for 24 h to allow the DOX to be encapsulated inside the pores of MSN. After that, the suspension was centrifuged at 10 000 rpm for 15 min and the supernatant was removed. The residual pellet was rinsed with DI water and redispersed into 2.0 mL of 50 mM HEPES buffer (1mM EDTA, pH=7.5) by sonicating for 2 min. The loading efficiency of DOX into MSN pores was determined by measuring changes in optical absorption of the feeding solution and supernatants at 490 nm. MSN loaded with CIS were prepared according to the previously reported procedure (Gu 2010). Briefly, 5 mg of CIS were dissolved in 5 mL of 1:1 H_2O:DMSO cosolvent (v:v) and 5 mg of pyridylthiol-terminated MSN were dispersed in the CIS solution by sonication. After 24 h stirring, CIS loaded MSN were centrifuged at 10 000 rpm for 15 min and the precipitated pellet was rinsed with DI water.

Quantification of CIS loading efficiency. Amount of CIS loaded into MSN was evaluated using a modified colorimetric assay based on the reaction of platinum with OPDA (Taylor 2010). Briefly, 1 mL of either CIS feeding solution or collected supernatant was mixed with 0.9 mL of 1.4 mg/mL OPDA dissolved in DMF. The mixture was heated to 110 °C for 10 min and then cooled in an ice bath for further 10 min. Furthermore, the mixture was diluted 10 times with DMSO and absorbance was measured at 720 nm. A calibration curve was constructed with solutions of known CIS concentrations in the range of 0.1-1.0 mg/mL. The percentage of loading was calculated as follows:

$$\% \text{ loading} = [(\text{Drug weight in MSN}) / (\text{MSN weight})] \times 100$$

Preparation of siRNA-conjugated (siRNA-MSN) MSN via disulfide linkage. 5’ thiol-siRNA targeted either to BCL2 or MRP1 mRNAs was obtained in a disulfide form. Prior to conjugation, the received siRNA was reduced using dithiothreitol (DTT) immobilized onto acrylamide resin (Reductacryl) according to the previously published procedure (Sun 2007). The siRNA and Reductacryl were first resuspended in water at a ratio of 1 mg siRNA to 50 mg resin to ensure complete reduction and the mixture was stirred at room temperature for 30 minutes. Reductacryl was finally removed by syringe filtration (pore size 0.2 μm). Furthermore, drug loaded MSN were reacted in 10 mM HEPES buffer (pH 8.5) with the reduced 5’ thiol-siRNA targeted either to BCL2 or MRP1 mRNA for 3 h. The final concentrations of MSN and 5’ thiol-siRNA in the reaction mixture were 1 mg/mL and 10 μM, respectively. The resulting siRNA-MSN conjugates were purified by centrifugation at 10 000 rpm for 10 min. The pellet was then collected, redispersed into DI H_2O, and centrifuged again at 10 000 rpm for 10 min. This centrifuge-redisperse cycle was repeated for a total of 4 times to remove any free siRNA. The amount of siRNAs conjugated to the surface of pyridylthiol-terminated MSN via disulfide bonds was quantified by measuring emission at 580 nm (excitation = 565 nm) of the dye such as TAMRA attached to the 5’ siRNA antisense strand. The release of siRNA from MSN as the result of disulfide bond cleavage was evaluated in the same manner as previously described (Taratula et al. 2009; Jung et al. 2010). Briefly, siRNA-MSN pellet resuspended in water was incubated with reduced glutathione at the concentration of 10 mM for 1 h at 37 °C. The resulting suspension was then centrifuged at 10 000 rpm for 10 minutes. The concentration of siRNA in the supernatant was evaluated by measuring emission of TAMRA dye at 580 nm using a Cary-Eclipse fluorescence spectrophotometer (Varian, Inv., Palo Alto, CA).

Synthesis of SH-PEG-LHRH conjugates. Heterobifunctional HS-PEG-COOH (5 kDa, Rapp Polymere GmbH, Tuebingen, Germany) was modified with LHRH peptide via amide bond formation according to our previously reported procedure (Chandna 2007). Briefly, the LHRH analogue, which has a reactive amino group only on the side chain of the lysine at position 6, was reacted with one equivalent of HS-PEG-COOH, in a mixture of anhydrous DMSO and DCM (3:5, v/v). Equimolar amount of EDC·HCl, was added as a coupling agent and DMAP was used as a catalyst. Triethylamine base was added to remove the salt from coupling agent. The reaction was stirred continuously for 24 h at room temperature. The resulting solution was filtered to remove dicyclohexylurea (DCU) and the filtrate was dialyzed extensively with DMSO and DI water (dialysis membrane of molecular weight cut off = 5 000 Da) for 24 h to remove unreacted LHRH peptide, EDC·HCl, DMAP and triethylamine. Furthermore, the conjugate was lyophilized.

Conjugation of LHRH-PEG-SH to siRNA-MSN. Drug loaded siRNA-MSN (concentration 1 mg/mL) were reacted in 10 mM HEPES buffer (pH 8.5) with thiol-modified PEG-LHRH (concentration 400 μM) for 3 h. The resulting product was purified by centrifugation at 10 000 rpm for 10 min and redispersed in DI water for further *in vitro* and *in vivo* studies. The presence of LHRH peptide conjugated to MSN was confirmed by bicinchoninic acid (BCA) protein assay according to our previously published procedure (Taratula et al. 2009). The BCA method employs the reduction of Cu^{+2} to Cu^{+1} by protein in an alkaline medium. The combination of BCA and Cu^{+1} creates a purple-collared product that absorbs at 562 nm. The amount of final product formed depends upon the amount of protein in the sample. Briefly, 20 μL of the test solution were mixed with 200 μL of working reagent and left to react for 30 min at 37 °C. The

solution then was incubated at room temperature for 10 min and the absorbance was measured at 560 nm.

Surface area, pore volume and pore size distribution. The surface areas, pore volumes, and pore size distributions of as-synthesized MSN and MPTS-modified MSN were analyzed by nitrogen adsorption/desorption techniques using accelerated surface area and porosimetry analyzer ASAP 2020 (Micromeritics, Norcross, GA) as previously described (Chen et al. 2009).

Particle size analysis. A Zetasizer Nano ZS90 (Malvern Instruments, UK) instrument was used to determine the size of the particles. All measurements were carried out at room temperature. Each parameter was measured five times, and average values and standard deviations were calculated.

Transmission electron microscopy (TEM). TEM imaging of MSN was performed using a Libra 120 TEM (Carl Zeiss, Thornwood, NY). A carbon coated 200 mesh copper grid was pre-rinsed with 5 µL of EtOH and then deposited with 5 µL of MSN suspension. After 3 minutes, the sample was drained off with a filter paper and further dried with a flow of N_2 gas. Then the sample was visualized using electron microscope and photographs were taken using a camera attached to the microscope.

Cell lines. A549 human lung adenocarcinoma cell line was obtained from the ATTC (Manassas, VA); A549 cells transfected with luciferase were purchased from Xenogen Bioscience,

(Cranbury, NJ). Cells were cultured in RPMI 1640 medium (Sigma Chemical Co., St. Louis, MO) supplemented with 10% fetal bovine serum (Fisher Chemicals, Fairlawn, NJ). Cells were grown at 37 ºC in a humidified atmosphere of 5% CO_2 (v/v) in air. All of the experiments were performed on the cells in exponential growth phase.

Cytotoxicity. The cellular cytotoxicity of all studied formulations of drugs and MSN was assessed using a modified 3-(4,5-dimethylthiazol-2-yl)-2,5-diphenyltetrazolium bromide (MTT) assay as previously described (Taratula 2011). Briefly, cancer cells were seeded into 96-well microtiter plates at the density of 10 000 cells per well. To measure cytotoxicity, cancer cells were separately incubated in a 96-well plate with different concentrations of MSN formulations, which resulted in a total of six separate series of experiments: (1) Control (fresh media); (2) MPTS-MSN; (3) LHRH-PEG-MSN; (4) Mixture of DOX and CIS (1:1, w/w); (5) Mixture of LHRH-PEG-DOX-MSN and LHRH-PEG-CIS-MSN (DOX/CIS = 1:1, w/w) and (6) Mixture of LHRH-PEG-siRNA(BCL2)-DOX-MSN, LHRH-PEG-siRNA(MRP1)-DOX-MSN, LHRH-PEG-siRNA(BCL2)-CIS-MSN and LHRH-PEG-siRNA(MRP1)-CIS-MSN (DOX/CIS = 1:1, w/w). Cells were cultured for 24 h before the cell viability assay was performed. The old medium was removed and 100 µl of fresh medium and 25 µl of a 5 mg/mL MTT (Sigma-Aldrich, Allentown, PA) solution in DPBS were added to each well. Plates were then incubated under cell culture conditions for 3 h. 100 µl of 50% (v/v) DMF in water containing 20% (w/v) sodium dodecyl sulfate (with pH adjusted to 4.7 by acetic acid) were added to every well and incubated overnight to dissolve the formazan crystals. The absorbance of each sample was measured at 570 nm with a background correction at 630 nm using a conventional microtiter plate reader. On the basis of

these measurements, cellular viability was calculated for each concentration of the formulation tested.

Cellular internalization of MSN. Fluorescent dye-labelled siRNA was synthesized by Invitrogen according to our design through the conjugation of TAMRA dye to the 5' siRNA antisense strand. The labeled siRNA possessed red fluorescence. Intrinsic fluorescent of DOX was employed for the detection of drug internalization into the cancer cells. In order to visualize cellular internalization of MSN with either siRNA or DOX, two different formulations were prepared: LHRH-PEG-siRNA(TAMRA)-MSN and LHRH-PEG-siRNA(non-labelled)-DOX-MSN. Prior to the visualization, A549 cells were plated (10 000 cells/well) in 6-well tissue culture plate and incubated with the studied formulations for 24 hr. In addition, cell nuclei were stained by a nuclear dye (4',6-diamidino-2-phenylindole, DAPI, Sigma Chemical Co., St. Louis, MO). Cellular internalization of LHRH-PEG-siRNA(TAMRA)-MSN and LHRH-PEG-siRNA(non-labelled)-DOX-MSN complexes were analyzed by a fluorescence microscope (Olympus America Inc., Melville, NY) as previously described (Taratula 2011).

Suppression of targeted mRNA. Quantitative reverse transcription-polymerase chain reaction (RT-PCR) was used for the analysis of the expression of genes encoding BCL2, MRP1 and β_2-*microglobulin* (β_2-*m*) proteins as previously described (Taratula 2011). Cancer cells were incubated within 24 h with following substances: (1) Control (fresh media); (2) Mixture of LHRH-PEG-DOX-MSN and LHRH-PEG-CIS-MSN, (3) Mixture of LHRH-PEG-siRNA(BCL2)-DOX-MSN, LHRH-PEG-siRNA(MRP1)-DOX-MSN, LHRH-PEG-siRNA(BCL2)-CIS-MSN and LHRH-PEG-siRNA(MRP1)-CIS-MSN (siRNA(BCL2):

siRNA(MRP1) =1:1); and (4) Mixture of LHRH-PEG-siRNA(BCL2)-MSN and LHRH-PEG-siRNA(MRP1)-MSN (siRNA(BCL2): siRNA(MRP1) =1:1). After incubation, RNA was isolated using an RNeasy kit (Qiagen, Valencia, CA). The total concentration of siRNA was 0.20 μM. First strand cDNA was synthesized by Ready-To-Go You-Prime First-Strand Beads (Amersham Biosciences, Piscataway, NJ) with 4 mg of total cellular RNA and 100 ng of random hexadeoxynucleotide primer (Amersham Bioscience, Piscataway, NJ). After synthesis, the reaction mixture was immediately subjected to the PCR, which was carried out using the GenAmp PCR System 2400 (Perkin-Elmer, Shelton, CT). The following pairs of primers were used: *BCL2* – GGA TTG TGG CCT TCT TTG AG (sense), CCA AAC TGA GCA GAG TCT TC (antisense); *MRP1* – ATG TCA CGT GGA ATA CCA GC (sense), GAA GAC TGA ACT CCC TTC CT (antisense); β_2-*m* (internal standard) – ACC CCC ACT GAA AAA GAT GA (sense), ATC TTC AAA CCT CCA TGA TG (antisense). PCR products were separated in 4% NuSieve 3:1 Reliant agarose gels in 1X TBE buffer (0.089 M Tris/Borate, 0.002 M EDTA, pH 8.3; Research Organic Inc., Cleveland OH) by submarine gel electrophoresis. The gels were stained with ethidium bromide, digitally photographed, and scanned using the Gel Documentation System 920 (NucleoTech, San Mateo, CA). Gene expression was calculated as the ratio of mean band intensity of analyzed RT-PCR product (*BCL2*) or *(MRP1)* to that of the internal standard (β_2-*m*). The value of *BCL2 and MRP1* genes expression for untreated cells (control) was set to 100%.

In vivo body distribution. Six week old NCR nude mice (20 g) were purchased from Taconic Farms, Inc. (Germantown, NY). A mouse orthotopic model of human lung cancer developed in our lab was used (Garbuzenko et al. 2010). Briefly, A549 human lung adenocarcinoma epithelial

cells transfected with luciferase (5–8 × 10^6) were resuspended in 0.1 mL of RPMI medium containing 20% FBS, mixed with 5 μM EDTA and administered intratracheally to the murine lung through a catheter. It was shown that a slight disruption of the pulmonary epithelium or the surfactant layer by co-administration of either pancreatic elastase or EDTA allowed significantly better tumour engraftment (March 2001). At the same time, cancer cell suspensions tolerate this concentration of EDTA, and animals subjected to EDTA at this concentration exhibit no histological pulmonary abnormalities. The progression of tumour growth was monitored by an IVIS (Xenogen, Alameda, CA) imaging system. Four weeks after the instillation of tumour cells, fluorescently labelled LHRH-PEG-siRNA-DOX-MSN formulation was administered into mice by inhalation or intravenous injection. The dose of the formulation containing DOX for both i.v. and inhalation administration was equal to 2.5 mg/kg. This dose corresponds to the maximum tolerated dose of free DOX. Animals were anesthetized with isoflurane using the XGI-8 Gas Anesthesia System (Xenogen, Alameda, CA). Fluorescence of labelled with Cy5.5 MSN was visualized 3 h after the injection using IVIS imaging system (Xenogen, Alameda, CA). Visible light and fluorescence images were taken and overlaid using the manufacturer's software to obtain composite images. The distribution of fluorescence in different organs was analyzed using original software developed in our laboratory.

Statistical analysis. Data were analyzed using descriptive statistics, single-factor analysis of variance (ANOVA), and presented as mean values ± standard deviation (SD) from four to eight independent measurements. The comparison among groups was performed by the independent sample student's *t*-test. The difference between variants was considered significant if $P < 0.05$.

Results

Synthesis and characterization of MSN

Herein, we report the synthesis of a targeted DDS for pulmonary co-delivery of anticancer drugs and suppressors of multidrug cellular resistance that is based on MCM-41 type of mesoporous silica nanoparticles. The MSN as drug delivery cargoes were synthesized and consequently modified with MPTS and Aldrithiol-2 to introduced pyridyldithiol reactive groups for covalent conjugation of multidrug resistance suppressors, PEG and targeting ligands (Fig.1A and 1B). DOX and CIS were used as the anticancer drugs to be encapsulated inside of the pyridyldithiol-terminated MSN (Fig.1C and 1D). Finally, the surfaces of the drug-loaded MSN were covalently modified with siRNA and PEG-LHRH via disulfide linkages (Fig.1E and 1F).

MCM-41 type MSN were synthesized using a surfactant-templated, base catalyzed condensation method, and were characterized by TEM, which showed a near spherical morphology with a hexagonal array of mesoporous channels (Fig. 2A). Furthermore, the surface areas, pore volumes, and pore size distributions of MSN were analyzed by nitrogen adsorption/desorption techniques. The Brunauer-Emmett-Teller (BET) surface area, the pore size and pore volume of nanoparticles determined using Barret-Joyner-Halenda (BJH) model are summarized in Table 1. As-synthesized MSN have an average pore size of 2.99 nm, surface area of 1001 m^2/g, and pore volume of 1.0 cm^3/g.

The mercaptopropyl-derivatized MSN were obtained by post-modification of as-synthesized MSN with MPTS, offering terminal thiol groups as reactive sites. Ellman's reagent was employed to quantify the concentration of thiol groups on the surface of MSN accessible for further modification. An average of 302.1 nmoles of thiols was measured per 1 mg of MSN via

standardization versus MPTS. As a result of MSN modification with MPTS, the average pore size, surface area and pore volume of MPTS-MSN were decreased to 2.83 nm, 821 m^2/g and 0.65 cm^3/g, respectively (Table 1). The DLS analysis revealed that MPTS-MSN had a uniform size around 160 nm with relatively low dispersion (Fig 2B).

In order to conjugate siRNA and PEG via disulfide linkages, the thiol groups on the surface of MSN were first reacted with Aldrithiol-2 to produce pyridyldithiol reactive groups. According to Ellman's reagent assay, after reaction with Aldrithiol-2, the free thiol groups on MSN surface were non-detected, which represent a fact that a majority of functional groups were activated and available for further conjugation with siRNA and PEG via reversible disulfide bond.

Loading of anticancer drugs inside the pores of pyridyldithiol-terminated MSN

In order to load DOX into the pores of MSN, our previously developed procedure was employed in the current study (Chen et al. 2009). Briefly, pyridyldithiol-terminated MSN were suspended in a DOX solution in 3:5 (v:v) MeOH:H_2O co-solvent under continuous stirring for 24 hr. After loading the suspension was centrifuged and DOX concentration in the supernatant was determined by UV-VIS spectroscopy (Chen et al. 2009). The difference between concentration of the drug in the feeding solution and supernatant was used to evaluate the amount of DOX loaded into the MSN. The encapsulation efficiency (weight ratio of loaded DOX to MSN carrier, w/w %) was determined by UV-Vis spectroscopy. To encapsulate CIS into the pores of nanoparticles, previously reported procedure was used in the current study (Gu 2010). Briefly, pyridyldithiol-terminated MSN were resuspended in CIS solution in 1:1 H_2O:DMSO cosolvent (v:v) under continuous stirring for 24 hrs. After centrifugation of MSN-CIS complexes, drug loading

efficiency was determined by using a modified colorimetric assay based on the reaction of platinum with OPDA. It was found that loading efficiency of DOX and CIS was approximately 8% and 30%, respectively.

Conjugation of siRNA and LHRH-PEG to MSN

To minimize the loss of siRNA activity, a thiol group was built into the sense strand of siRNA. This group was involved in the conjugation of siRNA to MSN via a thiol/disulfide exchange reaction. Briefly, 2-pyridyl activated thiol groups on the MSN surface at concentration of 302.1 μM reacted with 10 μM of thiol groups on 5' end of siRNA sense strand targeted either to BCL2 or MRP1 mRNA. To determine the efficiency of the conjugation method, the resulting siRNA-MSN were precipitated by centrifugation and the concentration of unconjugated siRNA in supernatant was evaluated by detecting emission of TAMRA dye on 5' end of an antisense strand. Calibration data were then employed to calculate the siRNA concentration left in the solution versus the covalently conjugated to the MSN surface. According to the obtained result, 80 % of siRNA molecules were covalently attached to MSN surface via disulfide linkage. The disulfide bond introduced between the MSN and siRNA is chemically labile and can be cleaved with a cell-produced disulfide reducing agent such as reduced glutathione releasing siRNA inside the cytoplasm. To confirm that the disulfide bonds of siRNA-S-S-MSN could be cleaved under cellular reductive conditions, the prepared conjugates were incubated for 30 min with 10 mM water solution of reduced glutathione at 37 °C, which corresponds to the concentration of reduced glutathione in the cellular cytoplasm (Anderson 1998). After centrifugation, the amount of siRNA in the supernatant was quantified by measuring emission of fluorescent dye (TAMRA)

attached to an antisense strand as described above. The obtained data demonstrated that 98% of siRNA was released from siRNA-S-S-MSN complex in the presence of reduced glutathione within 30 min. Based on this result, it is expected that the released siRNA could be involved in the RNAi mechanism without any loss of their activity. It is worth to mention, the antisense strands of siRNA used for *in vitro* and *in vivo* studies were not modified to preserve their biological functions.

In order to conjugate to nanoparticles via PEG polymer, the sequence of LHRH peptide was modified to provide a reactive amino group only on the side chain of a lysine residue. Therefore, primary amine of LHRH was first reacted with activated carboxylic group of heterobifunctional HOOC-PEG-SH. The purified LHRH-PEG-SH conjugates derivatized with a terminal sulfhydryl group were then added to the 2-pyridyl activated thiol groups on siRNA-Drug-MSN to obtain LHRH-PEG-siRNA-Drug-MSN complex via a sulfhydryl exchange reaction. It should be stressed that only 2.6 % of the 2-pyridyl activated thiol groups (8.0 nmole out of 302.1 nmole/1 mg of MSN) on MSN surface were used for conjugation of siRNA. Therefore, 97.4% (294.1 nmole/1mg of MSN) of the 2-pyridyl activated thiol groups were available for covalent attachment of LHRH-PEG-SH via disulfide linker. The presence of LHRH peptide on the MSN surface was confirmed by BCA protein assay (Thermo Fisher Scientific Inc., Rockford, IL). Additionally, DLS measurements revealed the fact that in comparison with non-modified MPTS-MSN, the modified LHRH-PEG-siRNA-Drug-MSN complex became slightly larger (from 160.0 nm to 180.0 nm for non-modified and modified nanoparticles, respectively) (Fig. 2B). The increase in the size of the prepared nanoparticles could be attributed to the modification of their surfaces by PEG and the targeting LHRH peptide layer.

In vitro cytotoxicity of nanoparticles

Cytotoxicity of a drug carrier is a major barrier for the efficient delivery of therapeutic agents. Whether the formulated non-targeted and cancer cell-targeted MSN influenced cell viability was investigated in A549 human lung cancer cells by MTT assay. The results of the measurements are shown in Figure 3A. One can see that over 90% of average cell viability was observed after incubation of cells with both MPTS-MSN (line 1) and LHRH-PEG-MSN (line 2) nanoparticles, at the concentrations which were used for *in vitro* experiment of the present study. Therefore, MSN in the concentrations used in the present study did not possess cellular toxicity.

Cellular internalization and extracellular localization of DOX and siRNA

To determine whether the MSN nanocarriers were able to efficiently deliver siRNA and anticancer drugs into cancer cells, the cellular internalization of both TAMRA-labelled siRNA and DOX delivered by nanoparticles was investigated by fluorescence microscopy (Fig. 4). In the typical experiment, LHRH-PEG-siRNA(TAMRA)-MSN and LHRH-PEG-siRNA(non-labelled)-DOX-MSN were incubated with A549 human lung cancer cells for 24 hrs and the appropriate visible light and fluorescence images were recorded using a fluorescence microscope. It should be stressed that after loading into the pores of MSN, DOX intrinsic fluorescence was completely quenched, which is in good agreement with our previous study (Chen et al. 2009). Moreover, the same results were observed for DOX encapsulated in liposomes and micelles and the phenomenon is attributed to a self-quenching effect of the drug (Gaber 1995; Kwon 1997). Consequently, the registered fluorescence of the drug inside the cells was attributed solely to the drug released from the nanoparticles. The above mentioned feature enables us to monitor the

release of active components from MSN-based DDS after cellular internalization. According to Figure 4, the developed DDS was capable to efficiently facilitate transfer of both siRNA (Fig. 4A-D) and DOX (Fig. 4E-H) through the cellular membrane. After incubation of A549 lung cancer cells with LHRH-PEG-siRNA (TAMRA)-MSN complexes, red fluorescence was detected in both cytoplasm and nuclei, indicating efficient intracellular delivery and release of siRNA from MSN (Fig 4A-D). On the other hand, following internalization DOX was predominately localized in the nuclear and perinuclear region of the cytoplasm (Fig. 4E-H).

Suppression of targeted mRNA

The ability of the siRNAs molecules delivered by MSN to silence the targeted mRNA was investigated using quantitative RT-PCR. The sequences of siRNA targeted to *BCL2* and *MRP1* mRNA were selected on the basis of our previously reported studies (Saad 2008). In the typical experiments, we measured the expression of targeted *BCL2* and *MRP1* genes in mRNA isolated from A549 human lung cancer cells incubated with a mixture of LHRH-PEG-siRNA(BCL2)-MSN and LHRH-PEG-siRNA(MRP1)-MSN (siRNA(BCL2): siRNA(MRP1) =1:1) for 24 hrs Untreated cells were used as controls. The results show that treatment with the developed complexes significantly influenced the expression of the *BCL2* and *MRP1* genes. Thus, at the studied conditions, 58% and 56% silencing were achieved for *MRP1* and *BCL2*genes, respectively (Fig.5A and 5B, lines 4). The obtained data support the conclusion that siRNA molecules were successfully released in cytoplasm from LHRH-PEG-siRNA-MSN complexes as a result of disulfide bond cleavage with reduced glutathione. Moreover, the released siRNA was available for the formation of RISC complexes for further gene suppression.

Anticancer efficiency of MSN-based DDS

Anticancer effect of the proposed MSN-based DDS that was capable of co-delivering anticancer drugs (cell death inducers) and siRNA (suppressors of pump and nonpump resistance) was studied *in vitro* using a modified MTT assay. It was found that a mixture of free antitumor drugs such as CIS and DOX at 1:1 w/w ratio substantially limited the viability of the cancer cells and cytotoxicity of anticancer agents increased with drugs concentrations (Fig. 3B, line 3). The complex of MSN with both drugs (Fig. 3B, line 4) demonstrated much higher cytotoxicity when compared with drugs alone (Fig. 3B, line 3) Remarkably, the mixture of both drugs and both siRNA delivered by LHRH-targeted MSN significantly enhanced their anticancer efficiency (Fig. 3b, line 5). According to MTT measurements, the IC_{50} dose (the dose that kills 50% of cells) of free drugs mixture (~9.0 μg/mL) was 6 times higher when compared to the mixture of CIS and DOX delivered by MSN based DDS (~1. 5 μg/mL, $P < 0.05$) specifically targeted to lung cancer cells. Therefore, the delivery of the same drug mixture by cancer-targeted nanoparticles significantly augmented their anticancer effect. The sufficient enhancement in cytotoxicity of anticancer agents is not caused by MSN alone since minimal toxicity for the drug-free nanoparticles at the employed concentrations was detected (Fig. 3A). The improved cytotoxicity of mixture of LHRH-PEG-DOX-MSN and LHRH-PEG-CIS-MSN can be explained by the possible higher accumulation of drugs inside the cells, which is in good agreement with our previous reports (Saad et al. 2008; Taratula et al. 2009). Furthermore, LHRH targeted MSN-drug complexes carrying both BCL2 and MRP1 siRNAs led to further enhancement of the antitumor

activity of CIS and DOX mixture (IC_{50}=0.3μg/mL, $P < 0.05$). The ability of the siRNAs to sufficiently enhance *in vitro* antitumor activity of CIS and DOX could be explained by decreasing both pump and nonpump drug resistances of cancer cells against chemotherapy. According to Figure 5 A (line 2) and 5 B (line 2), the expression of both MRP1 and BCL2 proteins responsible for pump and nonpump drug resistances increases after the treatment with anticancer drugs. Inhibition of pump resistance allows for increasing intracellular drug content while applying lower drug concentrations. However, even if drug efflux pumps are suppressed, cells still can survive high intracellular drugs concentrations due to the activation of nonpump resistance. Consequently, only simultaneous suppression of both types of cell resistance is capable to substantially increase the efficacy of anticancer drugs. Therefore, the above discussed effect was observed in the present study, when expression of MRP1 and BCL2 mRNAs responsible for pump and nonpump cellular resistance was downregulated by 50% and 35% respectively with apropriate siRNAs (Fig.5A and 5B, lines 3).

Organ distribution of MSN in vivo

Previously, we have shown (Garbuzenko et al. 2010) that for an efficient lung cancer treatment, the active ingredients of DDS should be locally delivered by inhalation to the lungs and retained there. In order to evaluate ability of the MSN-based DDS to provide local inhalation lung delivery of active components, previously developed instillation containing a Collison nebulizer connected to four-port, nose-only exposure chambers was used for inhalation co-delivery of the developed DDS into nude mice bearing an orthotopic murine model of lung cancer (Garbuzenko et al. 2010). The solution of LHRH-PEG-siRNA-DOX-MSN labelled with Cy5.5 was aerosolized at a flow rate of 2 L/min and then diluted by an additional 2 L/min air. Organ distribution of Cy5.5-labeled DDS was studied using the IVIS imaging system 3 h after a single

inhalation or i.v. administration. The data presented in Fig. 6 show that in comparison to i.v. administration, inhalation delivery substantially enhanced lung exposure to nanoparticles and limited the accumulation of complex MSN in other organs. Thus, the total amount of MSN retained in the lungs after inhalation (73%) was 14.6 times higher ($P < 0.05$) when compared to i.v. injection (5%). On the other hand, after intravenous (i.v.) administration the total content of MSN-based DDS per an entire organ was highest in liver (73%), kidneys (15%), and spleen (7%). While the amount of MSN-based DDS after single inhalation in liver, kidneys and spleen was 17%, 9% and 1%, respectively.

Discussion

In the present study, we describe the novel complex multifunctional drug delivery systems suitable for simultaneous tumour targeted inhalation delivery of several anticancer drugs in combination with various types of siRNA. The proposed treatment approach includes inhalation of a mixture (a cocktail) of several DDS. Every single DDS consists of a carrier (modified mesoporous silica nanoparticles), an anticancer drug (doxorubicin or cisplatin), a suppressor of pump or nonpump resistance (siRNA targeted to MRP1 or BCL2 mRNA) and a tumour targeting moiety (LHRH peptide). Each individual component of DDS performs its specific function. A carrier binds all other components together ensuring high water “solubility” of entire complex and effective penetration via plasma membranes of targeted cancer cells. An anticancer drug induces apoptosis in lung caner cells. Suppressors of pump and nonpump resistance inhibit active drug efflux from cancer cells and their antiapoptotic defence, respectively, substantially enhancing antitumor efficiency of anticancer drugs. A tumour targeting moiety guarantees the

uptake of an entire DDS with encapsulated drugs and siRNA specifically by cancer cells that express the corresponding receptor limiting adverse side effects on healthy lung cells. In addition, local inhalation delivery led to the preferential accumulation of delivered therapeutics mainly in the lungs and prevented the leakage of DDS and their components into the systemic circulation limiting adverse side effects of chemotherapy on healthy organs and tissues. We found that the mixture of four cancer targeted different DDS containing LHRH-PEG-siRNA(BCL2)-DOX-MSN, LHRH-PEG-siRNA(MRP1)-DOX-MSN, LHRH-PEG-siRNA(BCL2)-CIS-MSN, and LHRH-PEG-siRNA(MRP1)-CIS-MSN provides for a highest cytotoxic effect that cannot be achieved by either free drugs or drugs delivered by targeted MSN without siRNA. The components of DDS were selected based on the following considerations.

MSN as the drug carriers for inhalatory DDS have distinctive advantage over other nanocarriers. These nanoparticles have porous interiors that can be used as reservoirs for storing hydrophobic anticancer drugs and large surface areas that could be modified with siRNA and cell targeting moieties. The pore size can be tailored to selectively store different molecules of interest, while the size of the particles can be tuned to maximize the efficiency of pulmonary delivery, cellular uptake and ensuring the preferential accumulation of the lungs and preventing nanoparticle escape into the blood stream. In addition, a biodegradation product of MSN, orthosilicic acid, is a natural compound with low toxicity found in numerous human tissues (Perry 2009).

The selection of anticancer drugs in the current study was based on the following considerations. First, the drugs should be currently used in clinics for treatment of resistant non-small cell lung cancer. Secondly, experimental and clinical studies demonstrated that combinations of the anticancer drugs result in a more efficient tumour regression compared to

either drug alone (Muggia et al. 1997; Aziz et al. 1998; du Bois et al. 1999; Parra et al. 2001; Ahmed et al. 2006; Armstrong et al. 2006; Pinmai et al. 2008; Bilgi et al. 2010). Consequently, a mixture of DOX and CIS as the anticancer agents was selected for treatment of lung cancer via the pulmonary route.

siRNA has been shown to be highly effective in suppressing the synthesis of different proteins (Chen and Zhaori 2010; Guo et al. 2010; Laitala-Leinonen 2010; Shi et al. 2010; Tokatlian and Segura 2010). In order to suppress pump and nonpump resistance of lung cancer cells and therefore substantially enhance antitumor efficiency of delivered drugs, two types of siRNA were conjugated with MSN nanoparticles. The first type of siRNA was targeted to MRP1 mRNA. It is known that this protein is mainly responsible for active efflux anticancer drugs (pump resistance) in non-small cell lung carcinoma (Pakunlu et al. 2004; Xu et al. 2010). The second type of siRNA was targeted to BCL2 mRNA. This protein plays a central role in antiapoptotic defence forming the basis for nonpump resistance in many cancer cell lines and inhibition of such cellular defence can be effectively used in order to enhance the efficiency of chemotherapy (Pakunlu et al. 2003; Pakunlu et al. 2004; Pakunlu et al. 2006; Chen et al. 2009). Consequently, we expected that the use of siRNA targeted to MRP1 and BCL2 mRNA in the proposed DDS can provide for an effective suppression of both pump and nonpump cellular resistance and therefore enhance the effectiveness of anticancer drugs.

In order to improve steric stability of DDS and reduce its uptake by cells of reticuloendothelial system, heterobifunctional PEG was employed to modify the MSN surface with hydrophilic polymers. Moreover, the cytotoxic effect of chemotherapy on healthy organs can also be limited by employing the DDS with a ligand that specifically targeted to receptors overexpressed in the plasma membrane of cancer cells. Our previous study demonstrated that the

receptors for LHRH peptide are overexpressed in cancer cells and are not expressed detectably in most visceral organs (Dharap and Minko 2003; Dharap et al. 2003; Dharap et al. 2005). Taking advantage of this differential receptor expression, modified LHRH peptide was selected as targeting moiety for the proposed DDS to enhance drug uptake specifically by the lung cancer cells and limit the relative availability of the toxic drugs to normal cells in the lungs and other organs.

The investigation of synthesized targeted MSN showed that they were characterized by a narrow size distribution and were able to encapsulate both DOX and CIS. In addition, we were able to conjugate a tumour targeting moiety (LHRH peptide) and different siRNA molecules to the surface of the nanoparticles. The proposed DDS were able to effectively deliver their payload (anticancer drug and siRNA) into the cytoplasm preserving its specific activity. We found that both types of siRNA were able to significantly suppress the expression of targeted mRNA (MRP1 and BCL2) and delivered drugs effectively induced cell death. In fact, drugs delivered with tumour targeted MSN demonstrated higher cytotoxicity when compared with that of free drugs. This could be explained by the different mechanisms of cell internalization of free low molecular weight drugs and drug delivered by high molecular weight DDS targeted to the specific plasma membrane receptors (Mukherjee et al. 1997; Fotin-Mleczek et al. 2005; McNiven 2006; Bareford and Swaan 2007; Hillaireau and Couvreur 2009; Zaki and Tirelli 2010). It is well known that low molecular weight drugs are internalized by the cells via a “simple” diffusion. In non-small lung cancer cells these drugs are pumped out by the plasma membrane-bound drug efflux pumps, mainly attributed to the overexpression of MRP1 protein. Large molecular weight carriers containing a receptor-targeted moiety are internalized by receptor-mediated endocytosis in membrane limited organelles avoiding existing efflux pumps.

However, it is possible that a fraction of drugs delivered by tumour targeted DDS might be captured and effluxed by the pumps after their release from the DDS and diffusion out of endosomes or lysosomes. Therefore, the suppression of pump resistance is important even if the drugs are delivered by a targeted high molecular weight DDS. Such an assumption is supported by the experimental data obtained in the present investigation. We found that the combination of anticancer drugs with a suppressor of MRP1 protein significantly enhances their cytotoxicity. However, the cytotoxicity of anticancer drugs is also limited by the development a nonpump resistance. It is known that cellular antiapoptotic defence plays a central role in nonpump resistance. In turn, BCL2 protein is a major component of cellular defence mechanisms against apoptosis induction in many cancer cells (Gross et al. 1999; Reed 1999). Antiapoptotic cellular defence limits the activation of caspases on the response to the pro-apoptotic signal triggered by an anticancer drug and prevents the cell death. Consequently, BCL2 protein prevents drug-induced damage from being efficiently translated into the cell death. Therefore, the suppression of BCL2 protein should enhance cytotoxicity of simultaneously delivered anticancer drug(s). The data obtained in the present study fully support such a conclusion. We found that siRNA targeted to BCL2 mRNA delivered by MSN simultaneously with anticancer drugs significantly enhanced their cytotoxicity.

One major challenge of highly toxic anticancer therapeutics is their non-specific toxicity to healthy cells, tissues and organs which leads to severe adverse side effects of chemotherapy. The most effective approach for limiting such non-specific toxicity consist of the local delivery of cytotoxic agents specifically to the site of action, preventing their exit into the systemic circulation and targeting the delivery specifically to the cancer cells (Koshkina et al. 2001; Densmore 2003; Gautam and Koshkina 2003; Koshkina et al. 2003; Bunn 2004; Martins 2005;

Huang et al. 2010; Yi and Wiedmann 2010). In case of lung cancer, the anticancer agents should be delivered directly to the lungs by inhalation and a cancer specific targeting of DDS specifically to lung cancer cells should be employed to protect healthy lung tissues. The proposed MSN-based targeted DDS completely satisfies such requirements. It can be delivered by inhalation and incorporates a lung cancer-specific targeting moiety. The present experimental data showed that inhalatory delivery of the MSN led to their preferential accumulation in the lungs when compared with intravenous delivery of nanoparticles.

Conclusions

The developed complex MSN-based drug delivery system satisfies the major prerequisites for an effective treatment of lung cancer. This DDS can be locally delivered into the lungs limiting the penetration of nanoparticles into the systemic circulation and exposure to other healthy organs. The proposed system is able to deliver different anticancer drugs into lung cancer cells in combination with siRNA for a simultaneous induction of cell death and suppression of pump and nonpump cellular drug resistance. The drugs and siRNA delivered by the targeted MSN-based DDS preserve their specific activity. Moreover, simultaneous induction of cell death by anticancer drugs and suppression of pump and nonpump resistance by siRNA substantially enhances drugs cytotoxicity. Consequently, the proposed DDS has high potential in the effective treatment of lung cancer.

Acknowledgements

The research was supported in part by grants from the National Cancer Institute (R01 CA111766 and R01 CA138533) and the grant from the Department of Defence Lung Cancer Research Program (W81XWH-10-1-0347).

References

Ahmed F, Pakunlu RI, Brannan A, Bates F, Minko T, Discher DE. 2006. Biodegradable polymersomes loaded with both paclitaxel and doxorubicin permeate and shrink tumors, inducing apoptosis in proportion to accumulated drug. J Control Release 116:150-8.

Anderson ME. 1998. Glutathione: an overview of biosynthesis and modulation. Chem Biol Interact 112:1-14.

Armstrong DK, Bundy B, Wenzel L, Huang HQ, Baergen R, Lele S, Copeland LJ, Walker JL, Burger RA. 2006. Intraperitoneal cisplatin and paclitaxel in ovarian cancer. N Engl J Med 354:34-43.

Aziz Z, Zahid M, Ud Din Ahmed Z, Arshad T. 1998. Phase II trial of ifosfamide and cisplatinum in advanced ovarian cancer. Aust N Z J Med 28:403-9.

Bareford LM, Swaan PW. 2007. Endocytic mechanisms for targeted drug delivery. Adv Drug Deliv Rev 59:748-58.

Beck-Broichsitter M, Gauss J, Packhaeuser CB, Lahnstein K, Schmehl T, Seeger W, Kissel T, Gessler T. 2009. Pulmonary drug delivery with aerosolizable nanoparticles in an ex vivo lung model. International Journal of Pharmaceutics 367:169-178.

Bilgi O, Karagoz B, Alacacioglu A, Ozgun A, Tuncel T, Gokhan-Kandemir E. 2010. Irinotecan and cisplatin vs. cyclophosphamide, doxorubicin, and vincristine as second-line treatment after platinum and etoposide in small-cell lung cancer. J BUON 15:395.

Borm PJA, Kreyling W. 2004. Toxicological hazards of inhaled nanoparticles - Potential implications for drug delivery. Journal of Nanoscience and Nanotechnology 4:521-531.

Bravo-Osuna I, Teutonico D, Arpicco S, Vauthier C, Ponchel G. 2007. Characterization of chitosan thiolation and application to thiol quantification onto nanoparticle surface. International Journal of Pharmaceutics 340:173-182.

Bunn PA, Jr. 2004. Early-stage non-small-cell lung cancer: current perspectives in combined-modality therapy. Clin Lung Cancer 6:85-98.

Chandna P, Saad M, Wang Y, Ber E, Khandare J, Vetcher AA, Soldatenkov VA, Minko T. 2007. Targeted proapoptotic anticancer drug delivery system. Mol Pharm 4:668–678.

Chen AM, Zhang M, Wei DG, Stueber D, Taratula O, Minko T, He HX. 2009. Co-delivery of doxorubicin and Bcl-2 siRNA by mesoporous silica nanoparticles enhances the efficacy of chemotherapy in multidrug-resistant cancer cells. Small 5:2673-2677.

Chen SH, Zhaori G. 2010. Potential clinical applications of siRNA technique: benefits and limitations. Eur J Clin Invest 41:221-32.

Densmore CL. 2003. The re-emergence of aerosol gene delivery: a viable approach to lung cancer therapy. Curr Cancer Drug Targets 3:275-86.

Dharap SS, Minko T. 2003. Targeted proapoptotic LHRH-BH3 peptide. Pharm Res 20:889-96.

Dharap SS, Qiu B, Williams GC, Sinko P, Stein S, Minko T. 2003. Molecular targeting of drug delivery systems to ovarian cancer by BH3 and LHRH peptides. J Control Release 91:61-73.

Dharap SS, Wang Y, Chandna P, Khandare JJ, Qiu B, Gunaseelan S, Sinko PJ, Stein S, Farmanfarmaian A, Minko T. 2005. Tumor-specific targeting of an anticancer drug delivery system by LHRH peptide. Proc Natl Acad Sci U S A 102:12962-12967.

du Bois A, Neijt JP, Thigpen JT. 1999. First line chemotherapy with carboplatin plus paclitaxel in advanced ovarian cancer--a new standard of care? Ann Oncol 10 Suppl 1:35-41.

Fotin-Mleczek M, Fischer R, Brock R. 2005. Endocytosis and cationic cell-penetrating peptides--a merger of concepts and methods. Curr Pharm Des 11:3613-28.

Gaber MH, Hong K, Huang SK, Papahadjopoulos D. 1995. Thermosensitive sterically stabilized liposomes: formulation and in vitro studies on mechanism of doxorubicin release by bovine serum and human plasma. Pharm Res 12:1407-1416.

Garbuzenko OB, Saad M, Betigeri S, Zhang M, Vetcher AA, Soldatenkov VA, Reimer DC, Pozharov VP, Minko T. 2009. Intratracheal versus intravenous liposomal delivery of siRNA, antisense oligonucleotides and anticancer drug. Pharm Res 26:382-94.

Garbuzenko OB, Saad M, Pozharov VP, Reuhl KR, Mainelis G, Minko T. 2010. Inhibition of lung tumor growth by complex pulmonary delivery of drugs with oligonucleotides as suppressors of cellular resistance. Proceedings of the National Academy of Sciences of the United States of America 107:10737-10742.

Gautam A, Koshkina N. 2003. Paclitaxel (taxol) and taxoid derivates for lung cancer treatment: potential for aerosol delivery. Curr Cancer Drug Targets 3:287-96.

Gross A, McDonnell JM, Korsmeyer SJ. 1999. BCL-2 family members and the mitochondria in apoptosis. Genes Dev 13:1899-911.

Gu J, Su S, Li Y, He Q, Zhong J, Shi J. 2010. Surface modification−complexation strategy for cisplatin loading in mesoporous nanoparticles. J Phys Chem Lett 1:3446–3450.

Guo J, Fisher KA, Darcy R, Cryan JF, O'Driscoll C. 2010. Therapeutic targeting in the silent era: advances in non-viral siRNA delivery. Mol Biosyst 6:1143-61.

He QJ, Zhang JM, Shi JL, Zhu ZY, Zhang LX, Bu WB, Guo LM, Chen Y. 2010. The effect of PEGylation of mesoporous silica nanoparticles on nonspecific binding of serum proteins and cellular responses. Biomaterials 31:1085-1092.

Hillaireau H, Couvreur P. 2009. Nanocarriers' entry into the cell: relevance to drug delivery. Cell Mol Life Sci 66:2873-96.

Huang Y, Park YS, Wang J, Moon C, Kwon YM, Chung HS, Park YJ, Yang VC. 2010. ATTEMPTS system: a macromolecular prodrug strategy for cancer drug delivery. Curr Pharm Des 16:2369-76.

Jaracz S, Chen J, Kuznetsova LV, Ojima L. 2005. Recent advances in tumor-targeting anticancer drug conjugates. Bioorganic & Medicinal Chemistry 13:5043-5054.

Jung S, Lee SH, Mok H, Chung HJ, Park TG. 2010. Gene silencing efficiency of siRNA-PEG conjugates: Effect of PEGylation site and PEG molecular weight. Journal of Controlled Release 144:306-313.

Koshkina NV, Waldrep JC, Roberts LE, Golunski E, Melton S, Knight V. 2001. Paclitaxel liposome aerosol treatment induces inhibition of pulmonary metastases in murine renal carcinoma model. Clinical Cancer Research 7:3258-3262.

Koshkina NV, Waldrep JC, Knight V. 2003. Camptothecins and lung cancer: improved delivery systems by aerosol. Curr Cancer Drug Targets 3:251-64.

Kwon G, Naito M, Yokoyama M, Okano T, Sakurai Y, Kataoka K. 1997. Block copolymer micelles for drug delivery: loading and release of doxorubicin. J Control Release 48:195-201.

Laitala-Leinonen T. 2010. Update on the development of microRNA and siRNA molecules as regulators of cell physiology. Recent Pat DNA Gene Seq 4:113-21.

Lin YS, Tsai CP, Huang HY, Kuo CT, Hung Y, Huang DM, Chen YC, Mou CY. 2005. Well-ordered mesoporous silica nanoparticles as cell markers. Chemistry of Materials 17:4570-4573.

March TH, Marron-Terada PG, Belinsky SA. 2001. Refinement of an orthotopic lung cancer model in the nude rat. Vet Pathol 38:483-490.

Martins RG. 2005. Treatment of locally advanced non-small cell lung cancer with combination of chemotherapy and radiation. Semin Respir Crit Care Med 26:273-7.

McNiven MA. 2006. Big gulps: specialized membrane domains for rapid receptor-mediated endocytosis. Trends Cell Biol 16:487-92.

Melani AS. 2007. Inhalatory therapy training: a priority challenge for the physician. Acta Biomed 78:233-245.

Minko T, Dharap SS, Pakunlu RI, Wang Y. 2004. Molecular targeting of drug delivery systems to cancer. Curr Drug Targets 5:389-406.

Minna JD, Schiller, JH. 2008. Harrison's principles of internal medicine. McGraw-Hill. 551-562.

Molina JR, Yang PG, Cassivi SD, Schild SE, Adjei AA. 2008. Non-small cell lung cancer: Epidemiology, risk factors, treatment, and survivorship. Mayo Clinic Proceedings 83:584-594.

Muggia FM, Jeffers S, Muderspach L, Roman L, Rosales R, Groshen S, Safra T, Morrow CP. 1997. Phase I/II study of intraperitoneal floxuridine and platinums (cisplatin and/or carboplatin). Gynecol Oncol 66:290-4.

Mukherjee S, Ghosh RN, Maxfield FR. 1997. Endocytosis. Physiol Rev 77:759-803.

Nguyen J, Steele TW, Merkel O, Reul R, Kissel T. 2008. Fast degrading polyesters as siRNA nano-carriers for pulmonary gene therapy. J Control Release 132:243-251.

Pakunlu RI, Cook TJ, Minko T. 2003. Simultaneous modulation of multidrug resistance and antiapoptotic cellular defense by MDR1 and BCL-2 targeted antisense oligonucleotides enhances the anticancer efficacy of doxorubicin. Pharm Res 20:351-9.

Pakunlu RI, Wang Y, Tsao W, Pozharov V, Cook TJ, Minko T. 2004. Enhancement of the efficacy of chemotherapy for lung cancer by simultaneous suppression of multidrug resistance and antiapoptotic cellular defense: Novel multicomponent delivery system. Cancer Research 64:6214-6224.

Pakunlu RI, Wang Y, Saad M, Khandare JJ, Starovoytov V, Minko T. 2006. In vitro and in vivo intracellular liposomal delivery of antisense oligonucleotides and anticancer drug. J Control Release 114:153-62.

Parra HS, Tixi L, Latteri F, Bretti S, Alloisio M, Gravina A, Lionetto R, Bruzzi P, Dani C, Rosso R, Cosso M, Balzarini L, Santoro A, Ardizzoni A. 2001. Combined regimen of cisplatin, doxorubicin, and alpha-2b interferon in the treatment of advanced malignant pleural mesothelioma: a Phase II multicenter trial of the Italian Group on Rare Tumors (GITR) and the Italian Lung Cancer Task Force (FONICAP). Cancer 92:650-6.

Perry CC. 2009. An overview of silica in biology: its chemistry and recent technological advances. Prog Mol Subcell Biol 47:295-313.

Pinmai K, Chunlaratthanabhorn S, Ngamkitidechakul C, Soonthornchareon N, Hahnvajanawong C. 2008. Synergistic growth inhibitory effects of Phyllanthus emblica and Terminalia bellerica extracts with conventional cytotoxic agents: doxorubicin and cisplatin against human hepatocellular carcinoma and lung cancer cells. World J Gastroenterol 14:1491-7.

Radu DR, Lai CY, Jeftinija K, Rowe EW, Jeftinija S, Lin VSY. 2004. A polyamidoamine dendrimer-capped mesoporous silica nanosphere-based gene transfection reagent. Journal of the American Chemical Society 126:13216-13217.

Reed JC. 1999. Dysregulation of apoptosis in cancer. J Clin Oncol 17:2941-53.

Reference PD. 2007. Taxotere. Physicians Desk Reference 61:2932-2943.

Saad M, Garbuzenko OB, Ber E, Chandna P, Khandare JJ, Pozharov VP, Minko T. 2008. Receptor targeted polymers, dendrimers, liposomes: which nanocarrier is the most efficient for tumor-specific treatment and imaging? J Control Release 130:107-14.

Saad M, Garbuzenko OB, Minko T. 2008. Co-delivery of siRNA and an anticancer drug for treatment of multidrug-resistant cancer. Nanomedicine (Lond) 3:761-776.

Savla R, Taratula O, Garbuzenko O, Minko T. 2011. Tumor targeted quantum dot-mucin 1 aptamer-doxorubicin conjugate for imaging and treatment of cancer. J Control Release Epub ahead of print:

Shi Q, Zhang XL, Dai KR, Benderdour M, Fernandes JC. 2010. siRNA therapy for cancer and non-lethal diseases such as arthritis and osteoporosis. Expert Opin Biol Ther 11:5-16.

Slowing I, Wu CW, Vivero-Escoto JL, Lin VS. 2009. Mesoporous silica nanoparticles for reducing hemolytic activity towards mammalian red blood cells. Small 5:57-62.

Slowing II, Trewyn BG, Lin VSY. 2007. Mesoporous silica nanoparticles for intracellular delivery of membrane-impermeable proteins. Journal of the American Chemical Society 129:8845-8849.

Sun L, Yu C, Irudayaraj J. 2007. Surface-enhanced Raman scattering based nonfluorescent probe for multiplex DNA detection. Anal Chem 79:3981-3988.

Tao ZM, Xie YW, Goodisman J, Asefa T. 2010. Isomer-dependent adsorption and release of cis- and trans-platin anticancer drugs by mesoporous silica nanoparticles. Langmuir 26:8914-8924.

Taratula O, Garbuzenko OB, Kirkpatrick P, Pandya I, Savla R, Pozharov VP, He HX, Minko T. 2009. Surface-engineered targeted PPI dendrimer for efficient intracellular and intratumoral siRNA delivery. J Control Release 140:284-293.

Taratula O, Garbuzenko O, Savla R, Wang YA, He H, Minko T. 2011. Multifunctional nanomedicine platform for cancer specific delivery of siRNA by superparamagnetic iron oxide nanoparticles-dendrimer complexes. Curr Drug Deliv 8:59-69.

Taylor A, Krupskaya Y, Krämer K, Füssel S, Klingeler R, Büchner B, Wirth MP. 2010. Cisplatin-loaded carbon-encapsulated iron nanoparticles and their in vitro effects in magnetic fluid hyperthermia. Carbon 48:2327-2334.

Tokatlian T, Segura T. 2010. siRNA applications in nanomedicine. Wiley Interdiscip Rev Nanomed Nanobiotechnol 2:305-15.

Valle MJ, López FG, Navarro AS. 2008. Pulmonary versus systemic delivery of levofloxacin. The isolated lung of the rat as experimental approach for assessing pulmonary inhalation. Pulm Pharmacol Ther 21:298-303.

Valle MJD, Lopez FG, Hurle ADG, Navarro AS. 2007. Pulmonary versus systemic delivery of antibiotics: Comparison of vancomycin dispositions in the isolated rat lung. Antimicrobial Agents and Chemotherapy 51:3771-3774.

Vivero-Escoto JL, Slowing II, Trewyn BG, Lin VSY. 2010. Mesoporous silica nanoparticles forintracellular controlled drug delivery. Small 6:1952-1967.

Xu M, Sheng LH, Zhu XH, Zeng SB, Zhang GJ. 2010. Reversal effect of Stephania tetrandra-containing Chinese herb formula SENL on multidrug resistance in lung cancer cell line SW1573/2R120. Am J Chin Med 38:401-13.

Yi D, Wiedmann TS. 2010. Inhalation adjuvant therapy for lung cancer. J Aerosol Med Pulm Drug Deliv 23:181-7.

Youlden DR, Cramb SM, Baade PD. 2008. The international epidemiology of lung cancer - Geographical distribution and secular trends. Journal of Thoracic Oncology 3:819-831.

Yu J, Chien, YW. 1997. Pulmonary drug delivery: physiologic and mechanistic aspects. Crit Rev Ther Drug Carrier Syst 14:395-453.

Zaki NM, Tirelli N. 2010. Gateways for the intracellular access of nanocarriers: a review of receptor-mediated endocytosis mechanisms and of strategies in receptor targeting. Expert Opin Drug Deliv 7:895-913.

Figure legends

Figure. 1. Surface engineered approach for the preparation of mesoporous silica nanoparticles (MSN) for an efficient targeted co-delivery of siRNA and anticancer drugs. (A) Modification of MSN with MPTS; (B) Activation of thiol groups on the MSN surface with Aldrithiol-2 to produced pyridyldithiol reactive groups; (C) Encapsulation of DOX inside modified MSN; (D) Encapsulation of CIS inside modified MSN; (E) Modification of surface of CIS-loaded MSN with siRNA and PEG-LHRH; (F) Modification of surface of DOX-loaded MSN with siRNA and PEG-LHRH.

Figure 2. Characterization of mesoporous silica nanoparticles (MSN). (A) Transmission electron microscope image of as-synthesized MSN. (B) Size distribution of MPTS-MSN and LHRH-PEG-siRNA-DOX-MSN measured by dynamic light scattering.

Figure 3. Cytotoxicity of different formulations: (A) Mesoporous silica nanoparticles (MSN) without drugs; (B) Different drug formulations. A549 human lung cancer cells were incubated within 24 h with different concentrations of indicated formulations: 1 - MPTS-MSN; 2 - LHRH-PEG-MSN; 3 - Mixture of DOX and CIS (1:1 w/w); 4 - Mixture of LHRH-PEG-DOX-MSN and LHRH-PEG-CIS-MSN (DOX:CIS = 1:1 w/w); and 5 - Mixture of LHRH-PEG-siRNA(BCL2)-DOX-MSN, LHRH-PEG-siRNA(MRP1)-DOX-MSN, LHRH-PEG-siRNA(BCL2)-CIS-MSN and LHRH-PEG-siRNA(MRP1)-CIS-MSN (DOX:CIS = 1:1 w/w). Means ± SD are shown.

Figure 4. Representative fluorescent microscopy images of A549 human lung cancer cells incubated for 24 hrs with (A-D) LHRH-PEG-siRNA(TAMRA)-MSN and (E-H) LHRH-PEG-siRNA(non-labeled)-DOX-MSN . A and E represent light images of A549 cells; B and F represent fluorescence images of nuclei stained with DAPI. C and G represent cellular localization of siRNA and DOX, respectively. D and H are superposition of light and fluorescence images.

Figure 5. Representative images of RT-PCR products of MRP1 (A), BCL2 (B) and β_2-m (C and D, internal standard) mRNA and densitometric analysis of bands in A549 lung cancer cells incubated with following formulations: (1) Control (medium); (2) mixture of LHRH-PEG-DOX-MSN and LHRH-PEG-CIS-MSN; (3) mixture of LHRH-PEG-siRNA(BCL2)-DOX-MSN, LHRH-PEG-siRNA(MRP1)-DOX-MSN, LHRH-PEG-siRNA(BCL2)-CIS-MSN and LHRH-PEG-siRNA(MRP1)-CIS-MSN; and (4) Mixture of LHRH-PEG-siRNA(BCL2)-MSN and LHRH-PEG-siRNA(MRP1)-MSN. Gene expression in control was set to 100%. Means ± SD are shown. *$P < 0.05$ when compared with control.

Figure 6. Distribution of tumour targeted nanoparticles with siRNA and drugs in different organs after inhalation or intravenous administration. Nude mice bearing orthotopic human lung cancer were treated with Cy5.5-labeled LHRH-PEG-siRNA-DOX-MSN. Three hours after the treatment, fluorescence images of different organs were taken by IVIS imaging system and quantified. Panel A demonstrates representative fluorescence images of different organs. The intensity of fluorescence is expressed by different colours with blue colour reflecting the lowest intensity and red colour - highest intensity. Panel B demonstrates average relative content per an entire organ of labelled nanoparticles. Fluorescence intensity in each tissue is expressed as a percentage of the total.

Table 1. The Brunauer-Emmett-Teller (BET) surface area, the pore size and pore volume determined based on Barret-Joyner-Halenda (BJH) model. Means ± SD are shown.

Figures

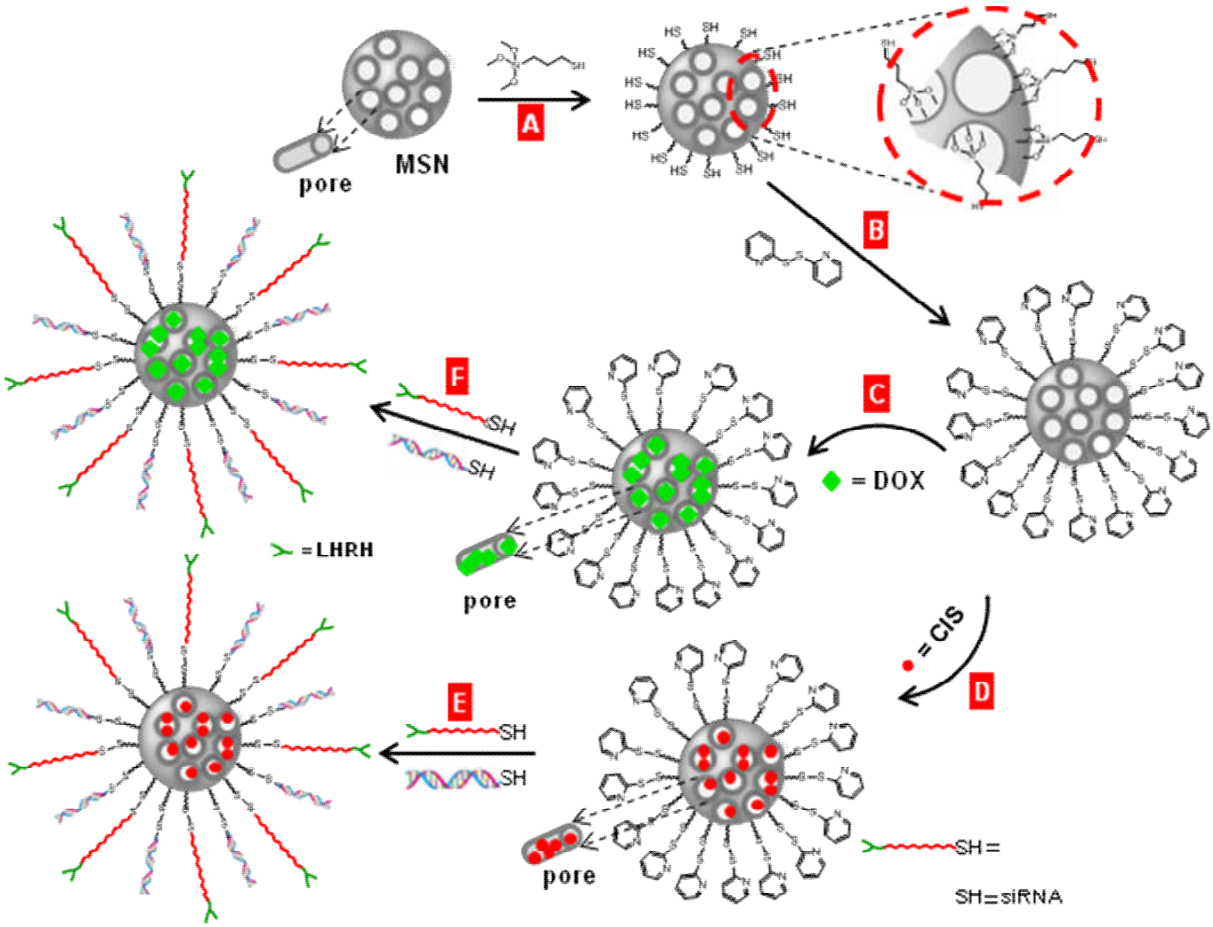

Figure 1.

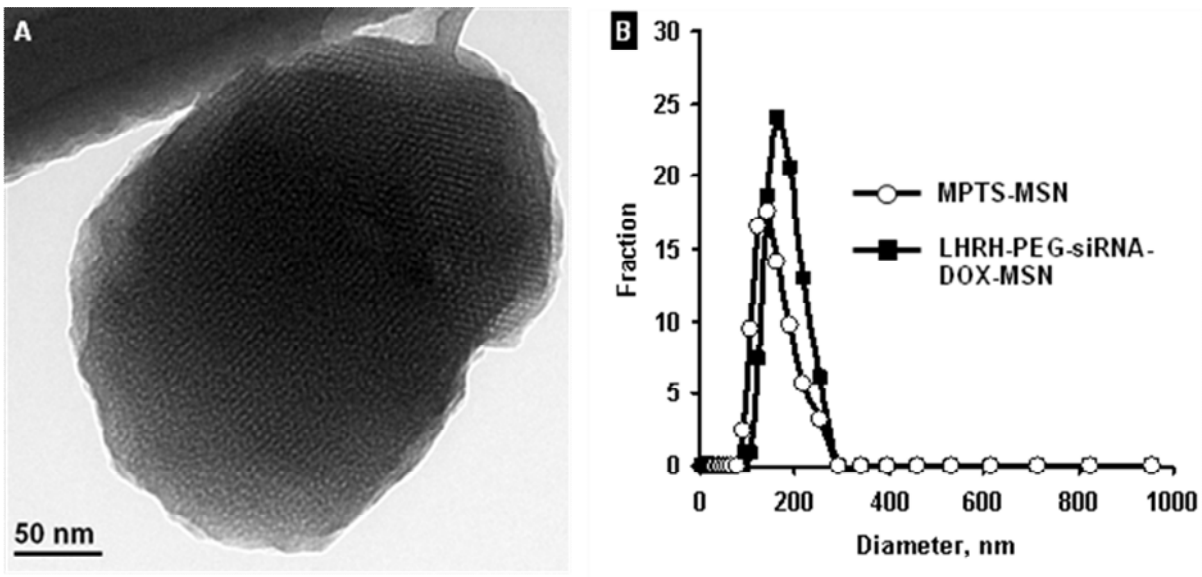

Figure 2.

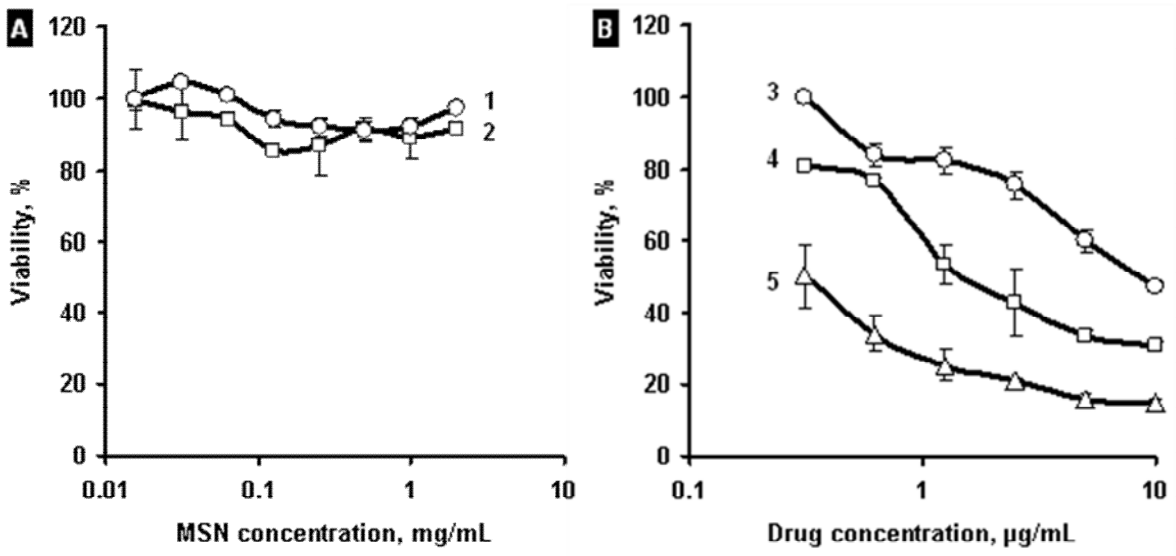

Figure 3.

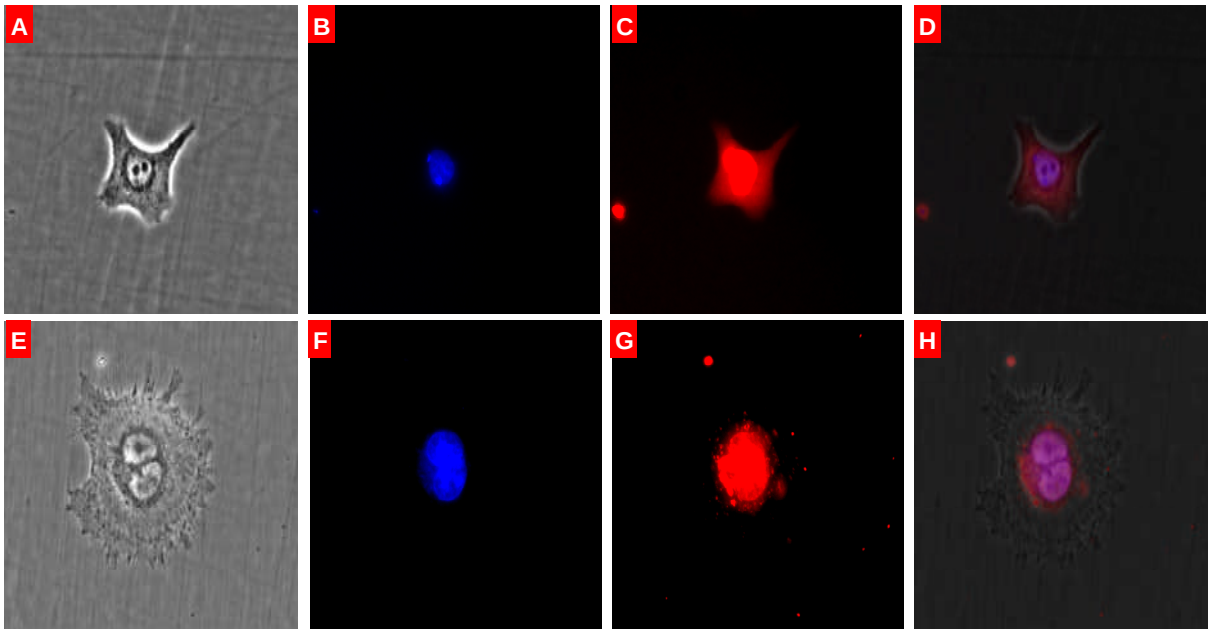

Figure 4.

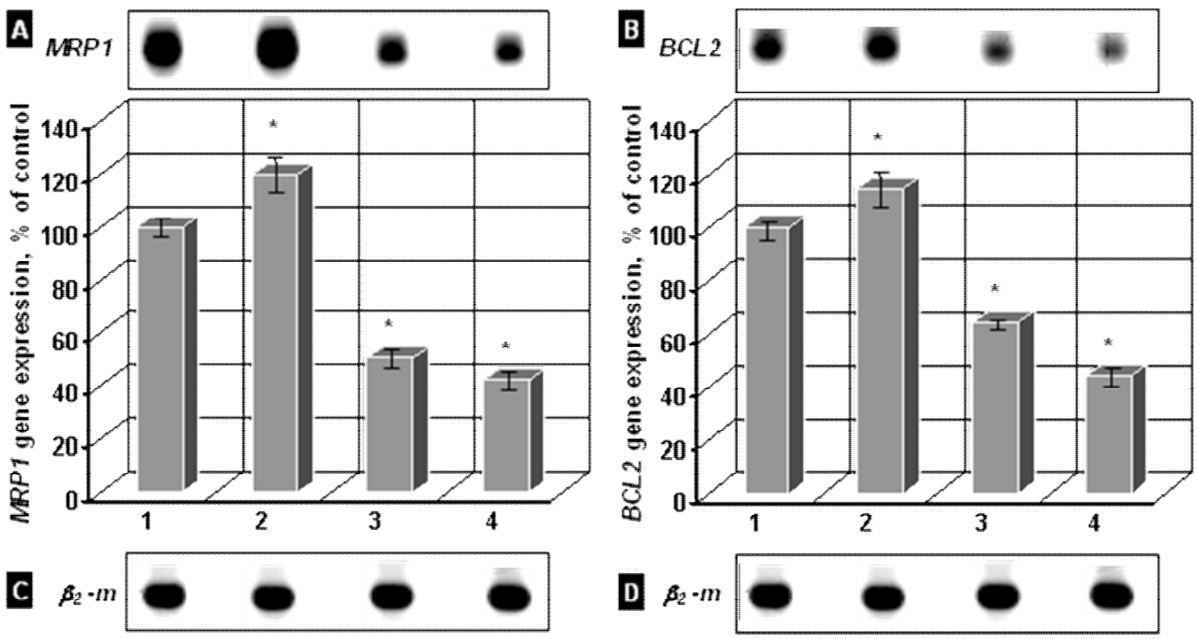

Figure 5.

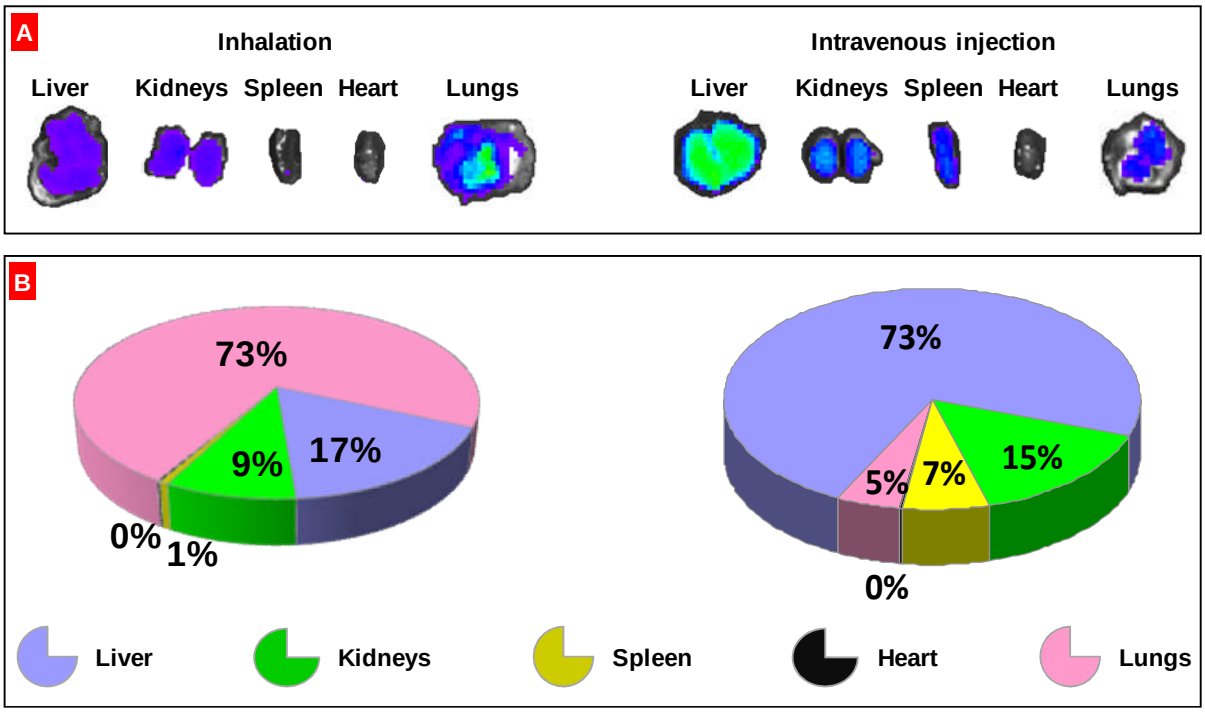

Figure 6.

Nanoparticle	BET surface area (m^2/g)	BJH pore volume (cm^3/g)	BJH pore size (nm)
MSN	1001 ±8	1.00 ±0.12	2.99 ±0.11
MPTS-MSN	821 ±5	0.65 ±0.06	2.83 ±0.08

Table 1.

Appendix B

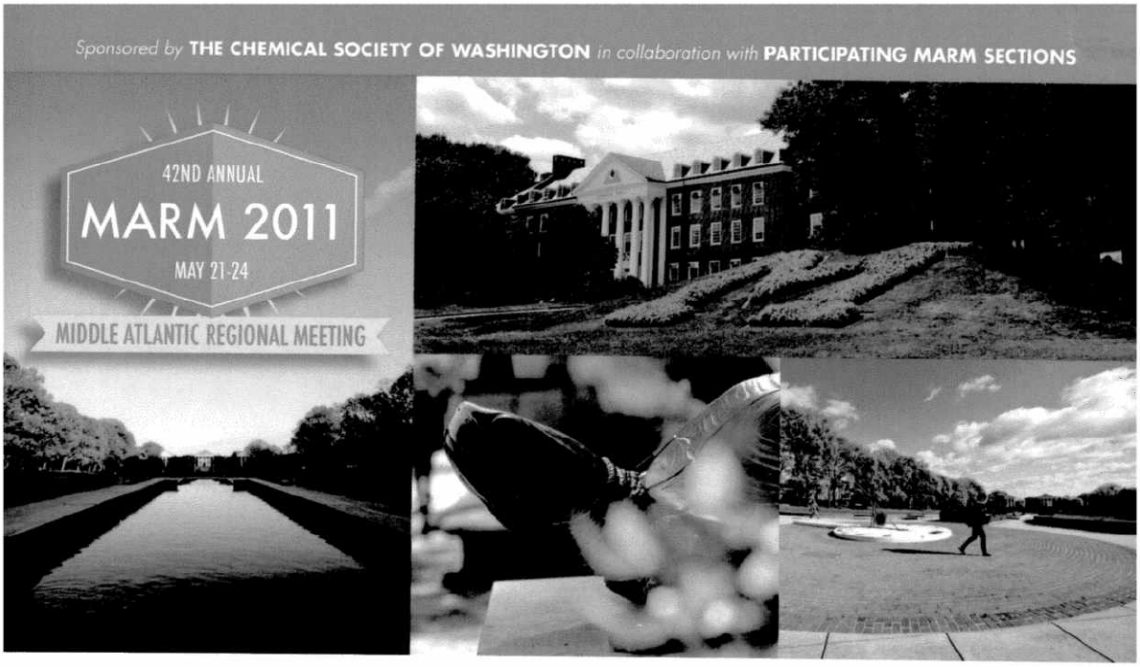

American Chemical Society
42nd Middle Atlantic Regional Meeting
at the University of Maryland, College Park, Maryland

MARM 2011 International Year of Chemistry

ACS Chemistry for Life™

IYC 2011 International Year of CHEMISTRY

UNIVERSITY OF MARYLAND

Appendix B

PROGRAM

Saturday, May 21, 2011 - Morning

Synthetic Chemistry across the Border

Metallation Chemistry
Stamp Student Union, Benjamin Banneker Room A
Organizers: P. Deshong, V. Snieckus

8:00 AM		Introductory Remarks.
8:05 AM	**4.**	Funtionalization of C(sp3)-H Bonds for Synthesis of Complex Molecules. **G. Chen**
8:40 AM	**5.**	Stereoselective Palladium-Catalyzed [2,3]-Stevens Rearrangement. **A. Soheili**, U. K. Tambar
9:00 AM	**6.**	Oxidative C-C bond formation mediated by a hypervalent iodine reagent: Developments and applications. **S. Canesi**
9:45 AM		Intermission.
10:00 AM	**7.**	1,2,3-Triazole: Unique ligands in metal coordination and catalysis. **X. M. Shi**
10:35 AM	**8.**	Progress Toward the Total Synthesis of Angustilodine, Alstilobanine A, and Alstilobanine E. **M. M. Majireck**, S. M. Weinreb
10:55 AM	**9.**	Synthesis of hetero-polycyclic compounds using formal [4+1]-cycloadditions. **C. Spino**, F. Beaumier, L. Boisvert, H. Rezaei, L. D.Lefebvre, M. Déry, K. Aissa
11:40 AM		Concluding Remarks.

Medicinal Chemistry and Chemical Biology of Anticancer Agents
Cosponsored by GVK BIO
Organizers: J. Talisman, S. Malhotra

8:15 AM		Introductory Remarks.
8:20 AM	**10.**	Caged nitric oxide (NO) prodrugs: A platform for broad-spectrum drug discovery. **L. K. Keefer**
8:50 AM	**11.**	D-peptide activators of the p53 tumor suppressor for anticancer therapy. C. Zhan, L. Zhao, X. Wu, W. Yuan, M. Pazgier, **W. Lu**
9:20 AM	**12.**	Advances in the anticancer properties of semisynthetic artemisinin dimers. **A. S. Rosenthal**, G. H. Posner
9:50 AM	**13.**	Small molecule modulation of the Lysophosphatidic acid pathway in the treatment of neoplastic growth. **J. E. East**, K. R. Lynch, T. L. Macdonald
10:20 AM		Intermission.
10:30 AM	**14.**	Design, synthesis, and biological evaluation of RSK inhibitors. **M. K. Hilinski**, B. Wu, G. A. O'Doherty, D. A. Lannigan

Appendix B

11:00 AM	**15.**	Innovative Strategy for Treatment of Lung Cancer: Inhalatory Co-Delivery of Anticancer Drugs and siRNA for Suppression of Cellular Resistance. **O. Taratula**, O. Garbuzenko, A. M. Chen, Z. Wang, G. Mainelis, T. Minko
11:30 AM	**16.**	Structure activity studies of antiproliferative factor: A novel glyocopeptide negative growth factor from interstitial cystitis patients. **J. J. Barchi**, K. M. Adams, S. Keay, P. Kaczmarek
12:00 PM		Concluding Remarks.

Chemical Education

New Approaches to Teaching Chemistry I
Stamp Student Union, Margaret Brent Room A
Organizer: S. Sinex

8:30 AM	**17.**	Teaching and learning in the digital age: Chemistry resources teachers and students can rely on from the ChemEd DL. **L. Fanis**, J. W. Moore
8:50 AM	**18.**	NMR determination of hydrogen bond thermodynamics in a dipeptide model: A physical chemistry experiment . **M. H. Schofield**, J. G. Morton, C. L. Joe, M. E. Chavez, S. R. Koshland, C. H. Londergan
9:10 AM	**19.**	Analysis of student performance on multiple-choice questions in general chemistry. **S. Lin**, J. R. Hartman
9:30 AM	**20.**	Dominant visuo-spatial techniques in the organic chemistry classroom. **B. C. Kumi**, R. Wroblewski, B. Dixon
9:50 AM	**21.**	Green chemistry educational materials and opportunities. **J. L. Young**
10:10 AM		Intermission.
10:25 AM	**22.**	Conceptual thinking versus plug-and-chug problem solving: Radiocarbon dating and interactive animated spreadsheets. **S. A. Sinex**, B. A. Gage
10:45 AM	**23.**	Description of a nontraditional freshman-sophomore chemistry sequence and an analysis of student performance. **R. J. Kashmar**
11:05 AM	**24.**	Woodward-Fieser rules on Excel spreadsheets. **R. A. Gross, Jr.**
11:25 AM	**25.**	Improving feedback from clicker questions. **D. B. King**
11:45 AM	**26.**	Dissecting the structure-mechanism-reaction paradigm of organic chemistry in a 100-student course with personal response systems ('clickers'): is 'structure' a threshold concept? **S. M. Graham**

Frontiers of Structure and Dynamics using NMR Spectroscopy

Protein Structure and Dynamics
Stamp Student Union, Charles Carroll Room A
Organizer: T. Dayie

8:30 AM		Introductory Remarks.
8:35 AM	**27.**	Detection of protein conformational Intermediates by NMR relaxation. **R. Ishima**

Appendix C

computer-aided docking studies. RSK is an unusual kinase, containing two functional, non-identical kinase domains, both an N-terminal (NTKD) and a C-terminal (CTKD) kinase domain connected by a linker. SL0101 is an ATP-competitive inhibitor of the NTKD of RSK, which is responsible for phosphorylation of exogenous substrates and belongs to the AGC kinase family. The closest relative of the RSK2 NTKD, p70 S6 kinase, adopts a canonical kinase structure that places an α helix (αC-helix), which contains residues important for the activation of ATP, near the ATP binding site. Interestingly, the crystal structure of the isolated active NTKD of RSK2 adopts a different conformation, in which a β-sheet displaces the αC-helix. This non-canonical crystal structure was used as the basis for docking studies of SL0101 and its analogues and was found to be consistent with known structure activity relationships and also predictive in the case of analogues that contain varying substitution at the 5″ position of the rhamnose portion of the molecule. This model is currently being used to develop analogues of SL0101 that would be suitable for evaluation in animal models of cancer.

15. Innovative Strategy for Treatment of Lung Cancer: Inhalatory Co-Delivery of Anticancer Drugs and siRNA for Suppression of Cellular Resistance

Oleh Taratula[(1)], *oleht@pegasus.rutgers.edu, 160 Frelinghuysen Road, Piscataway NJ 08854, United States ; Olga Garbuzenko*[(1)]*; Alex M Chen*[(1)]*; Zuocheng Wang*[(2)]*; Gediminas Mainelis*[(2)]*; Tamara Minko*[(1)]*. (1) Department of Pharmaceutics, Rutgers, The State University of New Jersey, Piscataway NJ 08854, United States (2) Department of Environmental Sciences, Rutgers, The State University of New Jersey, New Brunswick NJ 08901, United States*

Conventional chemotherapy usually employs high doses of toxic drugs which often induce severe adverse side effects on healthy organs. In addition, the efficacy of chemotherapy is also limited by the rapid development of tumor resistance. Therefore, to enhance lung cancer treatment, we developed an efficient nanomedicine platform based on Mesoporous Silica Nanoparticles (MSNs) for inhalation local delivery of anticancer drugs in combination with MRP1 and BCL2 targeted siRNAs as suppressors of pump and nonpump cellular resistance, respectively. Thiol-functionalized MSNs were synthesized by using a surfactant-templated, base-catalyzed condensation method by following post-modification of particle surface. The prepared particles have large surface areas (1000 m^2/g) and pore size (2.95 nm) that can be used as reservoirs for storing hydrophobic anticancer drugs. Doxorubicin was encapsulated into the pores of MSN, while thiol-functionalized siRNAs and polyethylene glycol (PEG) were chemically conjugated to the surface of MSNs via cleavable disulfide bonds. Furthermore, LHRH peptide was attached to the distal end of PEG to direct the delivery system (DS) specifically to the lung cancer cells and limit the cytotoxic effect of chemotherapy on healthy organs. *In vitro* study demonstrated the feasibility of the developed DS to sufficiently enhance delivery of Doxorubicin and siRNAs into human A549 lung cancer cells. Inhalation co-delivery of the developed DS into nude mice with an orthotopic model of human lung cancer substantially improved lung exposure to the active components and limited their accumulation in other organs when compared with intravenous administration. Moreover, targeting DS specifically to lung cancer cells enhanced the accumulation of DS in the lung tumor. Our results demonstrate high capability of MSNs to deliver their payload specifically to lung cancer tumor, substantially enhance the efficacy of lung cancer treatment and limit adverse side effects of chemotherapy on healthy organs.

16. Structure activity studies of antiproliferative factor: A novel glyocopeptide negative growth factor from interstitial cystitis patients

Joseph J Barchi[(1)], *barchi@helix.nih.gov, 376 Boyles Street, PO Box B, Frederick MD 21702, United States ; Kristie M Adams*[(1)]*; Susan Keay*[(2)]*; Piotr Kaczmarek*[(1)]*. (1) Chemical Biology, NCI Frederick, Frederick MD 21702, United States (2) Department of Medicine, University of Maryland, Baltimore MD 21202, United States*

Interstitial Cystitis/Painful Bladder Syndrome (IC/PBS) is a chronic bladder disorder characterized by severe pain caused by thinning and ulceration of the bladder wall. Interestingly, urine specimens from approximately 95% of IC/PBS patients contained an antiproliferative factor (APF) that induces